

## Article

# Modeling Land Use and Management Practices Impacts on Soil Organic Carbon Loss in an Agricultural Watershed in the Mid-Atlantic Region

Sadiya Baba Tijjani <sup>1</sup>, Junyu Qi <sup>2,\*</sup>, Subhasis Giri <sup>3</sup> and Richard Lathrop <sup>3</sup>

<sup>1</sup> Department of Geography, Rutgers, The State University of New Jersey, Lucy Stone Hall, 54 Joyce Kilmer Avenue, Piscataway, NJ 08854, USA; sadiya.baba@rutgers.edu

<sup>2</sup> Earth System Science Interdisciplinary Center, University of Maryland, 5825 University Research Ct, College Park, MD 20740, USA

<sup>3</sup> Department of Ecology, Evolution, and Natural Resources, School of Environmental and Biological Sciences, Rutgers, The State University of New Jersey, New Brunswick, NJ 08901, USA; subhasis.giri@rutgers.edu (S.G.); lathrop@crssa.rutgers.edu (R.L.)

\* Correspondence: junyuqi@umd.edu

**Abstract:** Measuring organic carbon (OC) losses from soils presents a challenge because of the intricate interplay of human-induced and biophysical processes. This study employs SWAT-C to simulate particulate OC (POC) and dissolved OC (DOC) losses from the Upper Maurice Watershed in the Mid-Atlantic Region. Simulation outcomes reveal that surface runoff was the primary contributor to the total DOC load (65%), followed by lateral flow (30%), and then groundwater (5%). Meanwhile, POC load was linked to erosion processes induced by surface runoff. Our findings indicate that agricultural land-use types exhibited the highest annual average DOC and POC loads. Forests and grasslands displayed intermediate loads, while barren land had the lowest load. Concerning seasonal fluctuations, agricultural land-use types exhibited distinct DOC and POC load patterns when compared to forest and grassland types, indicating the dominant role of management practices in determining soil OC (SOC) losses. Additional modeling of management practices' impact on SOC budgets indicates maximal SOC sequestration with full irrigation, no-till (NT), and full fertilization. In contrast, the largest SOC depletion arises from combining conservation tillage (CT) and no fertilization, irrespective of irrigation. This study shows that SWAT-C can be used to simulate land use and management impacts on SOC dynamics.

**Keywords:** particulate organic carbon; dissolved organic carbon; lateral carbon fluxes; SWAT model; carbon budget



**Citation:** Tijjani, S.B.; Qi, J.; Giri, S.; Lathrop, R. Modeling Land Use and Management Practices Impacts on Soil Organic Carbon Loss in an Agricultural Watershed in the Mid-Atlantic Region. *Water* **2023**, *15*, 3534. <https://doi.org/10.3390/w15203534>

Academic Editors: Manoj K. Jha, Philip W. Gassman, Raghavan Srinivasan and Ryan Bailey

Received: 15 August 2023

Revised: 23 September 2023

Accepted: 28 September 2023

Published: 10 October 2023



**Copyright:** © 2023 by the authors. Licensee MDPI, Basel, Switzerland. This article is an open access article distributed under the terms and conditions of the Creative Commons Attribution (CC BY) license (<https://creativecommons.org/licenses/by/4.0/>).

## 1. Introduction

Soil organic carbon (SOC) represents the largest C pool in terrestrial ecosystems and provides ecosystem services essential to human well-being [1]. Increasing SOC can enhance soil fertility, health, water infiltration, crop yield, soil structure, and moisture retention [2,3]. Maintaining SOC stocks in the terrestrial environment is of utmost importance for climate regulation, water supply regulation, nutrient cycling, erosion protection, and biodiversity enhancement [4].

There has been increased land conversion from natural vegetation to agricultural lands and the intensification of agricultural practices [5]. The growing human population has driven both land-use change and land-use intensification to meet global food, water, and energy demands, resulting in large energy and fertilizer consumption and considerable biodiversity loss [5]. Most importantly, converting forest or natural vegetation to agriculture can lead to an overall loss of SOC [6,7]. Once the soil is cultivated for agricultural production, soil organic matter (SOM) rapidly decomposes due to modifications in conditions such

as aeration, water content, and temperature [8]. Alterations in land use and management practices can impact soil functions that directly or indirectly connect with SOM, which can retain water and nutrients while providing additional ecosystem benefits [9,10]. Moreover, SOC balances are linked with C sequestration, while CO<sub>2</sub> emissions generated by OC decomposition raise atmospheric CO<sub>2</sub> concentrations, leading to global warming [11,12]. As a result, the SOC stock is considered a pivotal ecosystem service that aids in climate regulation [11].

Under long-term constant management and environmental conditions, agricultural SOC stocks are in a dynamic equilibrium between C inputs, mainly in the form of crop residues and losses of SOC as a result of (I) physical removal by surface runoff and erosion, (II) release of C into the atmosphere as CO<sub>2</sub> and CH<sub>4</sub>, and (III) leaching into the soil and groundwater [13,14]. SOC is lost from soils in water-dissolved OC (DOC) or sediment-bound OC, i.e., particulate OC (POC). The amount of DOC and POC exported from the terrestrial to aquatic ecosystem depends on many factors, such as the quality and quantity of litter and crop residue, manure, root exudates, and decomposition of OM [15]. In addition, anthropogenic activities such as farm management practices can increase the rate of DOC and POC losses through leaching to aquatic ecosystems [16]. Hydrological processes such as intense precipitation and runoff transport DOC and POC fluxes from terrestrial to aquatic ecosystems [17]. This can lead to water quality degradation and negatively impact human and aquatic ecosystems [18].

Comprehending the mechanisms that impact the flow of DOC and POC through diverse land uses and management approaches is crucial for forecasting the potential effects of forthcoming climate and/or land-use alterations on the well-being of terrestrial and aquatic ecosystems. Many studies have examined SOC losses using field experiments and measurement analyses [16,19,20]. However, field experiments and monitoring are time-consuming, expensive, and difficult to provide estimates of spatiotemporal variations in DOC and POC loads across different land-use types and management practices on the watershed scale. Such limitations in quantifying lateral OC fluxes also increase the uncertainty in total watershed C budget estimation [21,22].

Distributed eco-hydrological models can assist in filling the knowledge gap in understanding the impact of land use and agricultural activities on the quantity and quality of OM load by surface and sub-surface runoff and erosion [23,24]. Nevertheless, there are few watershed-scale models with the ability to simulate integrated OC cycling processes from terrestrial to aquatic environments. While these models can simulate SOC dynamics via the lateral transfer of POC and DOC from terrestrial ecosystems to aquatic bodies and through the carbon biogeochemical processes within river networks [23–28], they are not without their limitations. For instance, eco-hydrological models like the Integrated Catchments Model for Carbon (INCA-C) and the Regional Hydro-Ecological Simulation System (RHESSys) were designed to assess C fluxes from semi-natural vegetation [29,30] rather than cultivated watersheds, which limit their ability to capture fluxes from a more heterogeneous landscape. The Dynamic Land Ecosystem Model (DLEM; [31]) simulates nutrient fluxes from terrestrial to aquatic ecosystems at a global scale but does not address the spatial heterogeneity of various small watersheds.

To ascertain the sources/drivers of DOC and POC loads on a watershed scale and correlate them with the spatial and temporal distribution of diverse land-use categories and management strategies in our study area, we utilized an open-source eco-hydrological model, namely SWAT-C. This model is a refined version of the Soil and Water Assessment Tool (SWAT) [32], specifically developed to simulate C cycling processes in watersheds. The primary objectives of this study are as follows: (1) to evaluate the effects of distinct land-use types on POC and DOC loads in the Upper Maurice River Watershed (UMRW), New Jersey, which is a typical agricultural watershed in the Mid-Atlantic Region; (2) to explore the pathways for DOC and POC loads (e.g., surface runoff/sediment, lateral flow, and groundwater) and their seasonal variations across different land-use types; and (3) to

assess the influence of different management scenarios on SOC variations, as well as POC and DOC loads, and CO<sub>2</sub> emissions in the UMRW.

## 2. Materials and Methods

### 2.1. Study Area

The UMRW is located in southern New Jersey (Figure 1b) and is part of the Cohansey-Maurice Watershed (hydrologic unit code 02040206). The watershed is surrounded by several counties, including Salem (SAL), Gloucester (GLO), Atlantic (ATL), and Cumberland (CUM). The total watershed area covers approximately 445 km<sup>2</sup> and drains into the Delaware Bay watershed [33]. The watershed is selected due to its ecological and agricultural importance in the Delaware Bay watershed [34,35].

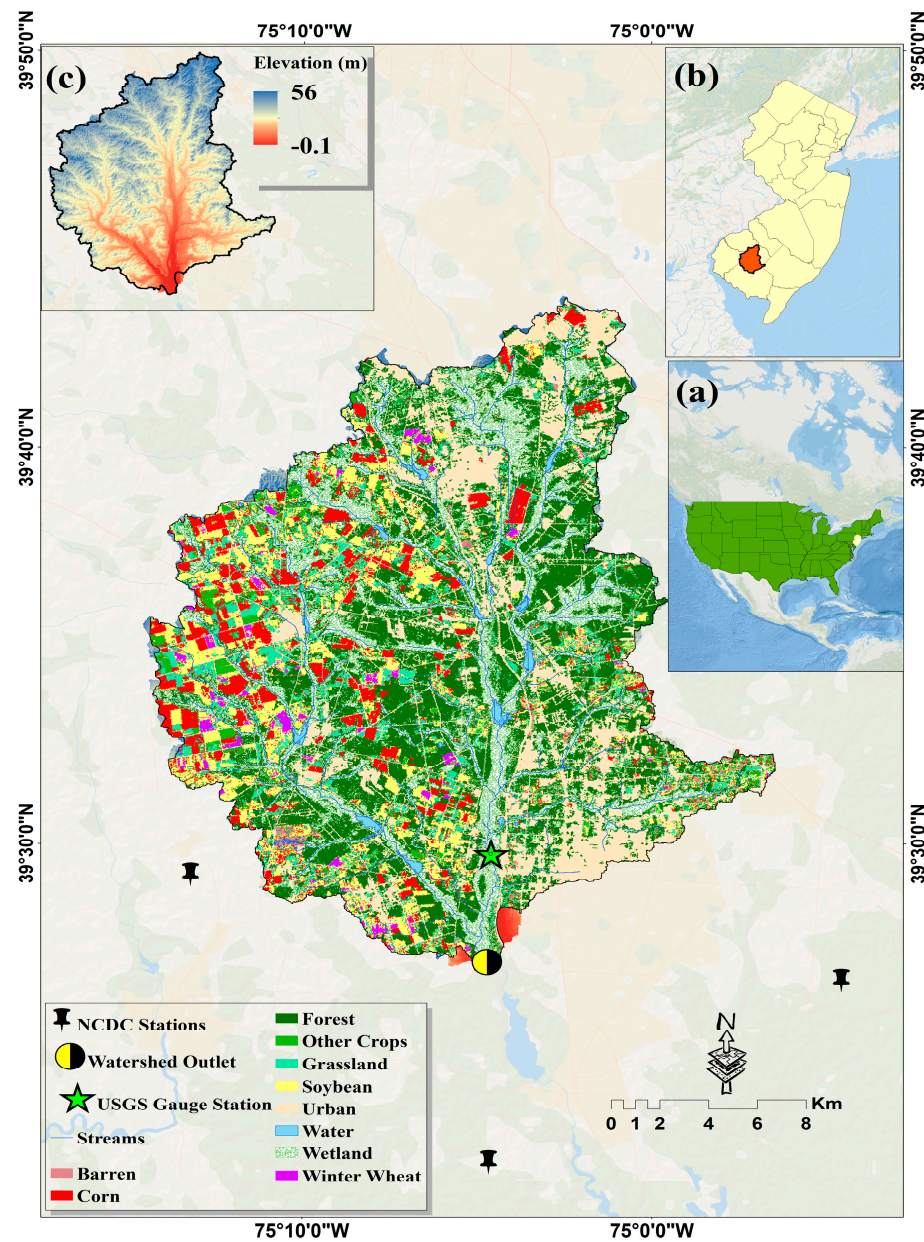


**Figure 1.** Location of the Upper Maurice River Watershed with respect to (a) the Mid-Atlantic region and (b) New Jersey. Also shown are (c) the elevation of the watershed and its land use and the USGS gauging station, weather stations, and watershed outlet.

Land use and land cover (LULC) data obtained from the U.S. Department of Agriculture (USDA) National Agricultural Statistics Service (NASS) have shown that the land in



In SWAT-C, SOM is typically categorized into five main pools: slow humus, passive humus, metabolic litter, structural litter, and microbial biomass. This categorization follows the DayCent model's structure but incorporates multiple soil layers instead of a singular integrated layer [18,46]. C and nitrogen (N) flow among these pools through various pathways influenced by biotic and abiotic factors (as shown in Figure 2). The rate of decomposition and transformation of C and N among the five pools is affected by factors such as soil temperature, soil water content, soil texture, land management, soil aeration, and soil conditions such as the soil C/N ratio [18,46]. C flow in the soil profile is associated with hydrological processes such as percolation, lateral flow, and erosion. Tillage and percolation can vertically redistribute SOM, while lateral flow and erosion redistribute SOM laterally. A schematic diagram of the cycling of OC from terrestrial to aquatic environments in SWAT-C is depicted in Figure 2. For more information regarding the transportation and transformation of OC, as well as management practice simulation in SWAT-C, please refer to previous studies (e.g., [18,45,47–50]) as well as supplementary information (see Text S3).

### 2.3. Model Setup, Calibration, Sensitivity, and Uncertainty Analysis

Fundamental inputs for the SWAT model encompass hydrography, topography, soils, land cover, and agricultural management practices. High-quality land-use data for the study area were obtained from the USDA NASS [51–53]. A 30 m digital elevation model (DEM) was obtained from the New Jersey Department of Environmental Protection [51]. Soil Survey Geographic Database (SSURGO) data downloaded from the USDA Natural Resources Conservation Services (NRCS) [53] represented the soil in the study watershed. Meteorological data consisting of daily precipitation and maximum/minimum temperature were obtained from the National Oceanic and Atmospheric Administration (NOAA) National Climatic Data Center (NCDC) for a period of 22 years (1999–2020) for three stations located close to the study watershed (Figure 1) [52]. A weather generator program embedded within SWAT generated solar radiation, relative humidity, and wind speed [54,55]. Table S2 lists management practices within the watershed. For model calibration and validation, we downloaded daily total suspended sediment (TSS), POC, and DOC concentrations in mg/l from the U.S. Geological Survey (USGS) [56] for 2001–2020. We then converted all three parameters into daily loads, where POC and DOC fluxes are in units of kg C/day, and sediment is in units of tons/day by multiplying each with the corresponding daily observed streamflow.

We divided the simulation period (2001–2020) into calibration (2001–2010) and validation (2011–2020) periods. A period of two years (1999–2000) was used as the warm-up period to initialize the SWAT simulation. A multistep calibration method was employed to calibrate the four water quality variables at a daily time step. First, we calibrated the streamflow, and then sediment and POC loads were calibrated together because the POC load is closely associated with sediment erosion, transportation, and deposition from land to stream networks [49]. Finally, the DOC load was calibrated. Table S3 lists all calibration parameters for daily streamflow, sediment, POC, and DOC loads in the UMRW. Model calibration was conducted with the SWAT Calibration and Uncertainty Program (SWAT-CUP) Premium version and the SWAT Parameter Estimator to find the optimum calibration parameters for daily streamflow, sediment, POC, and DOC loads [57].

To evaluate model performance, the Nash–Sutcliffe efficiency coefficient (NS; Equation (S10)) [58], the coefficient of determination ( $R^2$ ; Equation (S11)), and the percentage bias ( $P_{BIAS}$ ; Equation (S12)) were used [59]. We followed the model performance evaluation criteria outlined by Moriasi et al. [60]. We applied two indicators for the model uncertainty analysis, i.e., the  $p$ - and  $r$ -factors (Equations (S13) and (S14), respectively). The  $p$ -factor is the percentage of measured data bracketed by the 95% prediction uncertainty (95PPU), and the  $r$ -factor is the average thickness of 95PPU bands divided by the standard deviation of the observed data. For the  $p$ -factor, a value  $> 70\%$  for streamflow and a smaller value for sediment or other constituents is acceptable, while having an  $r$ -factor value of around one for streamflow and a larger value for sediment or other constituents is acceptable [60–62].

We used global sensitivity analysis, where parameter sensitivities were estimated by calculating multiple regression systems (Equation (S15)). The *t*-test was used to determine each parameter's relative significance through the inverse optimization approach [61]. Specifically, we followed three steps regarding the parameter sensitivities for POC and DOC loads specified by Qi et al. [49]: (1) a sensitivity analysis of the hydrological parameter for streamflow; (2) a sensitivity analysis of the sediment and POC parameters for the POC load; and (3) a sensitivity analysis of the DOC parameters for the DOC load.

Model performance evaluation during calibration and validation, along with sensitivity and uncertainty analyses, can be found in the supplementary information (see Text S5). Further model verification for agroecosystem carbon budgets was accomplished by employing crop yield data derived from USDA NASS, with detailed results illustrated in Text S9 of the supplementary information.

#### 2.4. Modeling Management Practice Impacts on SOC Budget

Our modeling strategy considered several commonly implemented management practices within the watershed, assessing their effects on biomass build-up, changes in SOC, soil microbial respiration (i.e., CO<sub>2</sub> emission), and lateral C losses in DOC and POC. Specifically, we explored combinations of these management practices to identify the most effective approach for increasing SOC storage while decreasing CO<sub>2</sub> emission and vertical and lateral C losses in the UMRW. Following Olson et al. [63], we developed two baselines (scenarios): (1) A pre-treatment baseline (i.e., baseline 1), representing the state of the soil before any treatment was administered (i.e., no irrigation, tillage, or fertilization). The pre-treatment baseline served as a reference to determine which treatment effectively sequestered CO<sub>2</sub> as SOC during 20 years of different management practices; (2) a post-treatment baseline (i.e., baseline 2), reflects current or conventional management practices wherein treatments were applied to the soil (see Table S2). By comparing the changes observed against baseline 2, we can recommend which management practices or combinations of practices should be adopted based on current conditions for maximum benefits. We identified 11 treatments with combinations of different levels of tillage (conventional vs. no-tillage), irrigation, and N fertilization (detailed in Table 1) for three crop rotations. We grouped the different treatments and presented the result based on three major categories and their subdivisions, i.e., (1) different fertilization levels with and without irrigation and tillage; (2) tillage with and without irrigation and fertilization, and (3) different irrigation levels with and without tillage and fertilization. These categories will be used to analyze the treatments compared to baselines 1 and 2.

Specifically, the first category is subdivided into three sub-categories, including:

- (1a) Treatment 3 vs. 4 vs. 5 vs. 9 (i.e., 0 N vs. −50% N vs. +50% N vs. shift in application date) under full irrigation and tillage;
- (1b) Treatment 7 vs. 8 (i.e., 0 N vs. full N) under NT and full irrigation;
- (1c) Treatment 1 vs. 10 (i.e., full N vs. 0 N) under CT with no irrigation.

The second category is divided into:

- (2a) Treatment 1 vs. 2 (i.e., no irrigation + CT + full N vs. no irrigation + NT + full N);
- (2b) Treatment 3 vs. 7 (i.e., full irrigation + CT + 0 N vs. full irrigation + NT + 0 N).

The third category is divided into:

- (3a) Treatment 1 vs. 6 (i.e., no irrigation + CT + full N vs. −50% irrigation + CT + full N);
- (3b) Treatment 3 vs. 10 (i.e., full irrigation + CT + 0 N vs. no irrigation + CT + 0 N);
- (3c) Treatment 2 vs. 8 (i.e., no irrigation + NT + full N vs. full irrigation + NT + full N).

It is worth noting that we developed a dynamic N fertilizer use scheme in treatment 9 following Lu et al. [64]. Considering that corn is included in all three rotations and is associated with the largest N fertilizer consumption (Table S2), we used two of its critical growth phases known as V1 (heat unit between 232 to 282) and V5 (heat unit between 496 to 546) for N fertilizer application. The fertilizer amount remains the same as the conventional

practice, but each growth phase receives 50% of the total annual amount applied between May and June instead of April.

**Table 1.** Lists management treatments in two scenarios for the three crop rotations.

No.	Treatments	Description	References
1	Treatment 1	No irrigation + CT + full N	[65,66]
2	Treatment 2	No irrigation + NT + full N	[67]
3	Treatment 3	Full Irrigation + CT + 0 N	[68]
4	Treatment 4	Full Irrigation + CT + (−50%) N	[69]
5	Treatment 5	Full Irrigation + CT + (+ 50%) N	[70]
6	Treatment 6	(−50%) Irrigation + CT + full N	[71]
7	Treatment 7	Full Irrigation + NT + 0 N	[70]
8	Treatment 8	Full Irrigation + NT+ full N	[68]
9	Treatment 9	Shifting fertilizer application date + Full irrigation + CT	[66]
10	Treatment 10	CT + 0 N + 0 Irrigation	[67]
11	Current management	Full irrigation + CT + full N	[72]

Note: CT = conservation tillage; NT = no tillage; N = nitrogen fertilizer.

### 3. Results and Discussion

Figure 3 and Table S7 show the annual water yield and sediment, POC, and DOC loads for the UMRW from 2001 to 2020. The watershed's annual POC load varied from 1.3 to 15.1 kg ha<sup>−1</sup> y<sup>−1</sup> (averaging ~5 kg ha<sup>−1</sup> y<sup>−1</sup>). The maximum POC load reported in our study was during Hurricane Irene (~15 kg ha<sup>−1</sup> y<sup>−1</sup>; Table S7) in 2011. The value reported here is close to that reported (11.3 kg ha<sup>−1</sup> y<sup>−1</sup>) by Caverly [20] in an agricultural watershed in the Chesapeake Bay during the same extreme event. Annual DOC loads averaged over the watershed ranged between 13.8 and 65 kg ha<sup>−1</sup> y<sup>−1</sup> from 2001 to 2020 (averaging ~27 kg ha<sup>−1</sup> y<sup>−1</sup>). The average DOC load reported here is slightly larger than the average annual DOC load (22 kg ha<sup>−1</sup> y<sup>−1</sup>) reported by Caverly [20]. The average annual DOC load determined in this study substantially exceeded the POC load, suggesting that the amount of dissolved OM transported from uplands was approximately five times that of particulate OM (with a DOC: POC ratio of ~5:1). The ratio of DOC to POC loads demonstrates substantial variance in disparate environments, including various ecosystems like forests, wetlands, and grasslands, as well as in differing climate conditions such as arid, tropical, and temperate zones. Additionally, this variability is affected by the presence of different soil types, land-use and land-cover changes, hydrological conditions, and anthropogenic activities like agriculture and urban development. Furthermore, variations in precipitation patterns, temperature regimes, and nutrient availability can also significantly impact the DOC to POC ratios in different environmental settings. For example, Lasanta et al. [72] reported that dissolved material is 70 times greater than the total suspended sediment load in an agricultural watershed in Las Bardenas, Spain. Furthermore, Li et al. [73] found that only 18% of the total OM load comprises suspended OM, while 81% of the total OM is composed of dissolved OM in two small basins in northern Pennines, UK.

We analyzed the correlation between annual POC/DOC loads and water yield and sediment load from 2001 to 2020. Pearson's correlation shows a robust relationship between the DOC load and water yield ( $R^2 = 0.89$ ;  $p < 0.05$ ; Figure 4a). The largest ten water years (i.e., years with above-average water yield) accounted for 65% of the total DOC load in the watershed for the 20-year study period. In a similar study, Li et al. [73] reported that variations in water yield could explain 95% of DOC load. Wallin et al. [74] observed a significant correlation between annual variation in precipitation/discharge and DOC load. A positive relationship between water yield and POC load shows that runoff can explain

77% of POC load in the UMRW (Figure 4c;  $p < 0.05$ ) less than sediment load, which can explain 87% of POC load (Figure 4b). Other studies have reported a similar relationship between runoff and sediment load and POC load [74,75]. For example, Michalzik et al. [76] found that increased sediment erosion and water yield generally lead to higher lateral C fluxes in temperate regions.

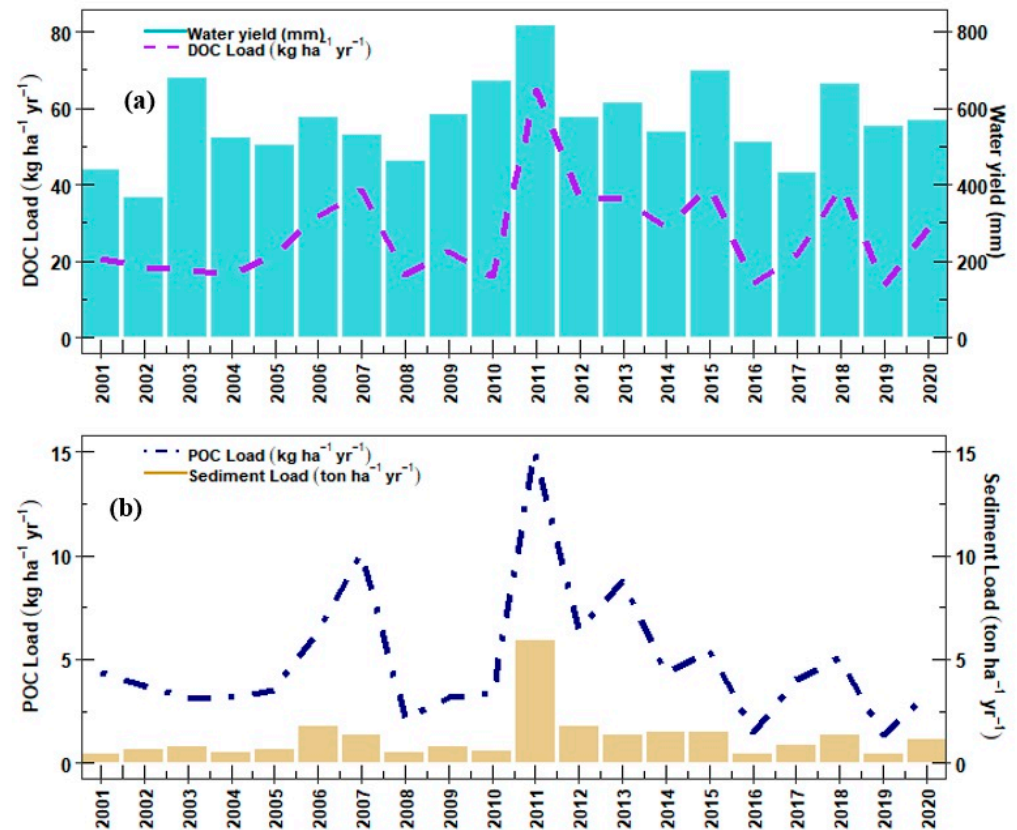


**Figure 3.** (a) Annual variation in water yield (mm) vs. DOC load (kg/ha) and (b) sediment yield (ton/ha) vs. POC load (kg/ha) in the UMRW.

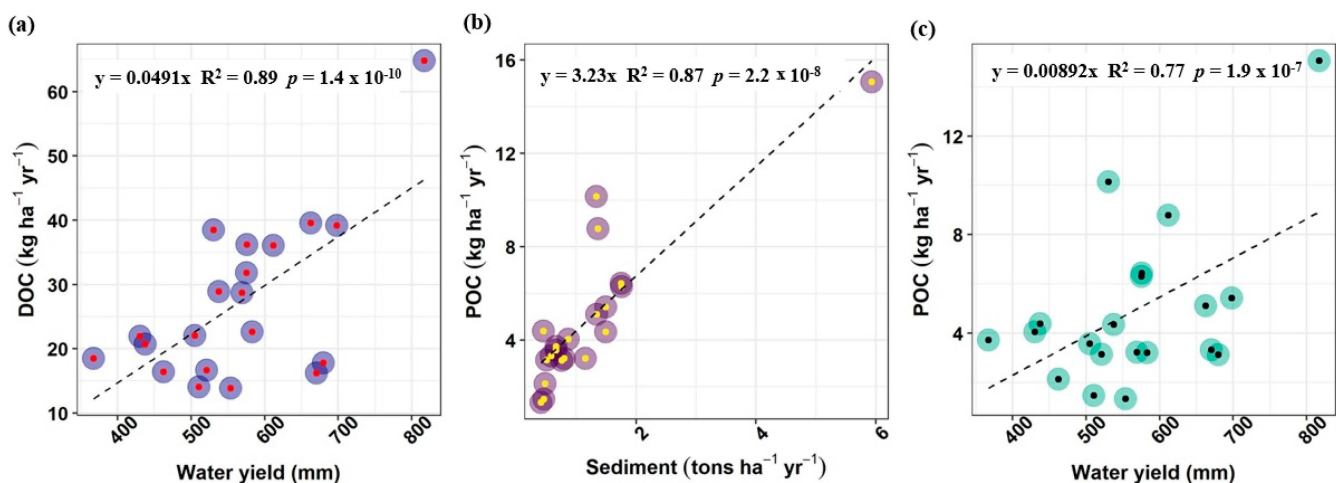


**Figure 4.** Scatter plots of annual (a) DOC load vs. water yield, (b) POC load vs. sediment yield, and (c) POC load vs. water yield from 2001 to 2020 in the UMRW.

### 3.1. Impact of Land Use on POC and DOC Fluxes

We employed the Tukey’s HSD (honest significant difference) test to estimate the average annual POC and DOC contributions from various land-use types in the UMRW

based on simulations from 2001 to 2020 (Tables S8 and S9; Figure 5). Our results show that agricultural land-use types, including CS, CSS, and other crops, produced the highest and comparable DOC loads, corresponding to an annual average of 20, 21, and 21 kg ha<sup>-1</sup> yr<sup>-1</sup>, respectively. Forest, grassland, and CSW produced comparable annual DOC loads corresponding to 16, 17, and 17 kg ha<sup>-1</sup> yr<sup>-1</sup>, respectively. In contrast, barren land generated the lowest DOC load (0.1 kg ha<sup>-1</sup> yr<sup>-1</sup>; Figure 5a). Furthermore, agricultural land-use types, including CS (2.6 kg ha<sup>-1</sup> yr<sup>-1</sup>), CSS (2.6 kg ha<sup>-1</sup> yr<sup>-1</sup>), CSW (2.3 kg ha<sup>-1</sup> yr<sup>-1</sup>), and other crops (3.3 kg ha<sup>-1</sup> yr<sup>-1</sup>), generated greater POC loads than forest (0.5 kg ha<sup>-1</sup> yr<sup>-1</sup>), grassland (1 kg ha<sup>-1</sup> yr<sup>-1</sup>), and barren land (<0.5 kg ha<sup>-1</sup> yr<sup>-1</sup>; Figure 5b). It is noteworthy that the discrepancies in DOC load between agricultural land-use types and forest and grassland are considerably more pronounced than those for POC load. This suggests that the impact of land-use change on POC is more pronounced than on DOC, owing to the soil conservation characteristics inherent to forests and grasslands.

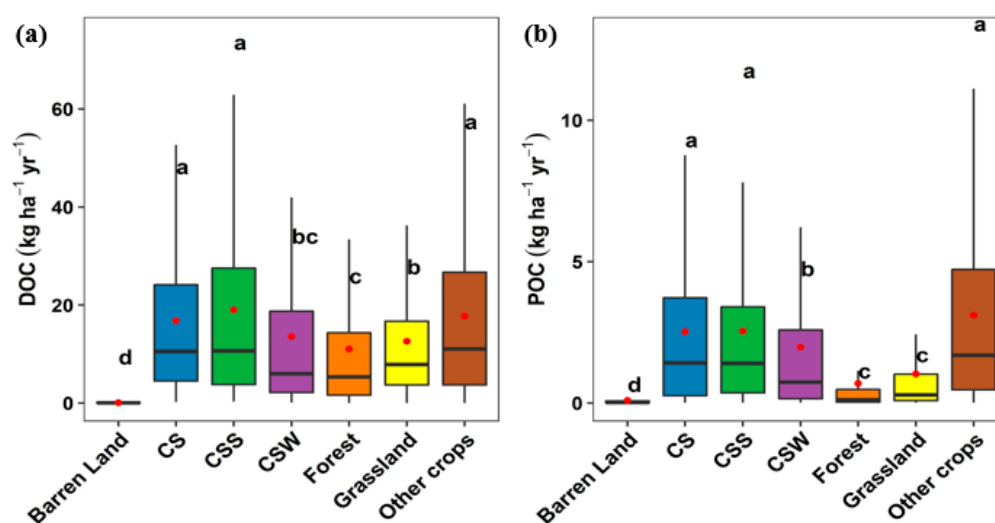


**Figure 5.** Boxplots of average annual (a) DOC and (b) POC loads for different land-use types simulated from 2001 to 2020. The boxplot's red dot represents the annual mean, while the black horizontal line shows the median value. Boxes with the same letter above them are not significantly different. Tables S7 and S8 provide full details of the analysis.

The variation in DOC and POC loads over the different land-use types depends on several factors, including quality and quantity of organic residue input (e.g., lignin content and C: N ratio), temperature, soil moisture, management practices, soil texture, hydrological conditions, among others [77–79]. Barren land generates the highest runoff but the least DOC and POC loads among all land-use types because of its low residue input and SOM content [79]. Overall, agricultural land-use types generated higher DOC and POC loads compared to forests and grasslands, emphasizing the prominent role of agricultural intensification and management practices in SOC losses [5]. For instance, Lupwiya et al. [79] found that 40% of wheat residue and 45–55% of pea residue decomposes faster in conventional tillage management compared to 27% and 43% in no-tillage. The low contribution of POC by forests and grassland is related to their soil conservation properties, such as erosion control. Zahedifar [80] also reported a lower soil quality and resistance index in cultivated land compared to forests and grasslands. Many studies have documented the positive impact of natural vegetation on soil conservation and C sequestration [81–83]. Glover et al. [84] and Jackson et al. [85] reported that higher microbial diversity, rooting depth, and mass leads to higher SOC content in grassland rather than cropland. Notably, CSW produces lower DOC/POC loads in comparison to other agricultural land-use types. This is likely attributable to the additional tillage post-soybean harvest (Table S2), which reduces surface OM, the primary source for generating

both DOC and POC. This suggests that management practices have a substantial impact on the losses of SOC within agroecosystems [86].

### 3.2. DOC Flow Pathways and Seasonal Variations

DOC is transported from land to the river network through surface runoff, lateral flow, and groundwater flow. Generally, surface runoff is the primary source of year-round total DOC load, contributing approximately 65% to the total load. This is not surprising, considering DOC flux depends on discharge rates and OM enrichment, which are more prevalent in the topsoil layer [73]. Several studies have reported that the largest concentration of total C was found in the surface soil layer due to litter fall, residue accumulation, rhizodeposition, and dead microbial turnover [87,88]. Our analysis shows lateral flow was a secondary source of total DOC load, contributing approximately 30% to the total load. Groundwater provided the lowest DOC load (about 5%) in the watershed. Our result is consistent with findings from other studies. For instance, Sobczak et al. [89] reported that most DOC loads were found in surface and lateral flows instead of groundwater. Low DOC loads in the groundwater can be attributed to the microbial metabolism of DOC obtained from freshwater recharge [89]. Siemens [90] also reported that the DOC load could decrease by 78–84% as it moves from 90 cm to a soil depth of 3–5.6 m.

We computed the seasonal sum (i.e., three-month sum) of water yield and DOC loads for different land-use types across the three pathways (Figure 6). Consistent with annual analysis results, the seasonal total DOC load patterns across various land-use types generally aligned with water yield patterns, except for summer and barren land. Although groundwater contributed a secondary water yield, it supplied the lowest DOC load across various land-use types in various seasons. Forest and grassland DOC loads exhibited a similar seasonal pattern, with higher values in spring and summer and lower values in fall and winter, corresponding to temperature fluctuations that influence decomposition rates [91,92]. Conversely, the DOC load seasonal pattern for agricultural land-use types differed from those of forests and grasslands and exhibited variations among the different agricultural land-use types. For instance, CSS had the highest DOC loads during fall and winter (23% and 28%, respectively;  $p < 0.05$ ; Figures S5a and 6), while other crops exhibited the highest DOC loads during summer and spring (25% and 21%, respectively;  $p < 0.05$ ; Figures S5a and 6). The availability of CSS residue and soybean's low C: N ratio may explain why CSS exhibits the highest load during fall and winter [93]. For instance, Begum et al. [94] found that C losses in residues with low lignin content, such as soybean, are higher than in residues with high lignin content. The high contribution of other crops to the DOC load in summer can be attributed to multiple factors. These include the presence of freshly added residue left on the surface without tillage, a low C: N ratio (refer to the list of other crops in Table S1), warmer temperatures (Figure S4), and soil moisture due to spring/summer precipitation, which contribute to an accelerated decomposition rate [76,87]. Notably, the seasonal DOC load for CSW differed from that of CS and CSS, particularly during the spring and summer months when CSW generated distinctly lower DOC loads (Figure 6). This can be attributed to the additional tillage practices undertaken prior to the planting of winter wheat (Table S2) [95].

Overall, the contrasting seasonal patterns of DOC loads for agriculture and other land-use types indicated the dominant role of management practices in determining DOC losses. The findings also demonstrate the capability of the SWAT-C model to simulate SOC pools and losses following seasonal variations and management practices.

### 3.3. Seasonal Variation in POC Fluxes

Compared to DOC load, the POC transportation pathways are simpler and are primarily associated with erosion and sediment load correlated with surface runoff (Figure 4b,c). In Figure 7, we present the seasonal sum (i.e., three months sum) of POC loads from 2001 to 2020 for various land-use types during the four seasons. Generally consistent with the annual results (Figure 5), agricultural land-use types generated significantly higher POC loads

compared to barren land, forest, and grassland across all seasons (Figures S5b and 7) [96]. This outcome is expected since forests and grasslands produce less erosion due to better surface soil protection [97]. In contrast, barren land generated high surface runoff and erosion rates (Figure 6) but low POC load (Figure 7) due to low OM content [3].

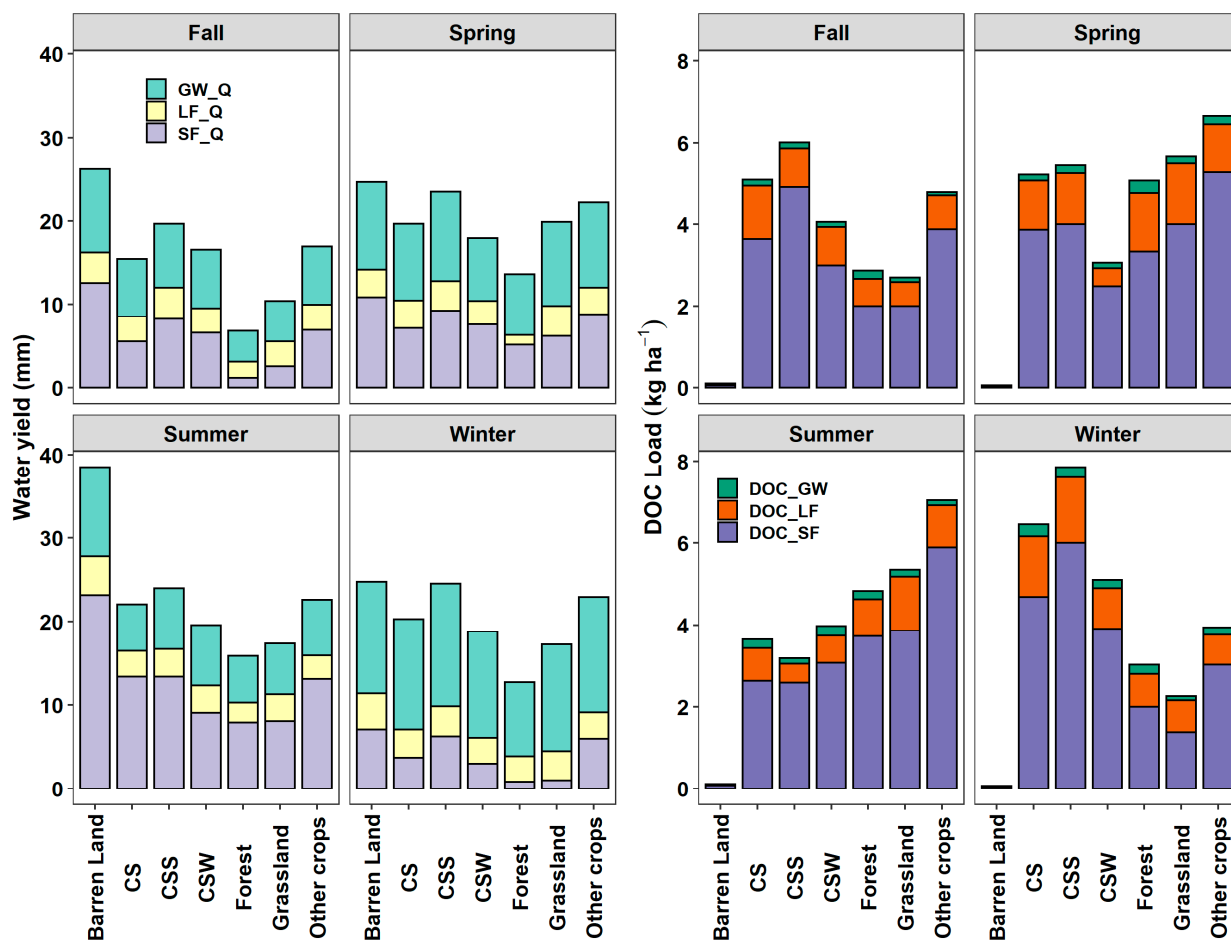


**Figure 6.** Seasonal groundwater (GW\_Q), surface runoff (SF\_Q), and lateral (LF\_Q) flow, and DOC loads via groundwater (DOC\_GW), lateral flow (DOC\_LF), and surface runoff (DOC\_SF) for different land-use types. Fall: September to November. Spring: March to May. Summer: June to August. Winter: December to February. Values represent the total for each season, accumulated over three months.

The seasonal patterns of POC load differed among the four agricultural land-use types (Figures 7 and S5b), particularly for CSW and other crops. CSW produced lower POC loads during winter (Figures 7 and S5b) compared to other agricultural land-use types. Besides the impact of tillage on the redistribution of surface residue (Table S2), winter wheat serves as a cover crop, protecting the soil surface from erosion throughout its growth period in the winter season. Analogous to the DOC load, the other crop land-use types generated increased POC loads during summer. The lack of tillage operations leads to residue accumulation on the soil surface, making them more susceptible to erosion (see Tables S1 and S2). Moreover, the CSS rotation led to a higher POC load during winter, implying a propensity for soybean decomposition during the colder seasons due to its low C: N ratio. The resulting insufficient soil coverage may have contributed to sediment erosion.

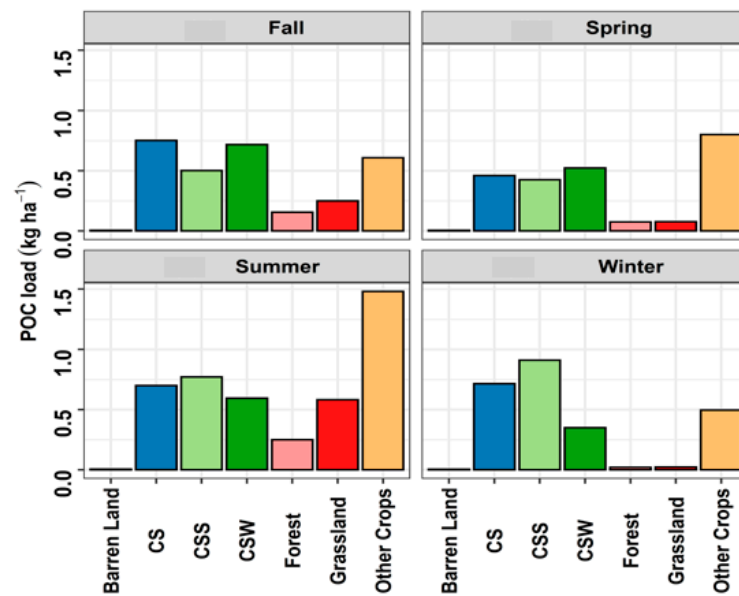


**Figure 7.** Seasonal POC loads for different land-use types. Fall: September to November. Spring: March to May. Summer: June to August. Winter: December to February.

### 3.4. Management Practice Impacts on SOC Budget

Upon examining two management scenarios, we observed that SOC increased in treatments 2, 5, 8, and 9 across all three rotations compared to both baselines. The only common practice among these four treatments is full N (+50% N for treatment 5). The second common practice, full irrigation, and NT did not show a consistently positive impact on SOC. On the contrary, SOC decreased in treatments 3, 4, and 10 across all three rotations compared to both baselines. The shared practices for these three treatments are 0 N (−50% N for treatment 4) and full irrigation. Generally, SOC change corresponded with changes in biomass, the major controlling factor. No evident negative correlation was found between respiration CO<sub>2</sub> and SOC change. For POC and DOC loads, the change patterns were complex. In the subsequent sections, we delve deeper into the effects of individual practices on SOC budgets.

#### 3.4.1. Scenario 1 Analysis

##### Fertilization Effects

Under sub-category (1a; see Section 2.4 for explanation), treatment 9 has the highest SOC sequestration in each rotation (CS: 1.44 ton/ha (+1.4%), CSS: 0.3 ton/ha (+0.23%), and CSW: 2.23 ton/ha (+2.3%);  $p$ -value < 0.05; Figure 8i; Table S10), while treatment 3 has the most significant negative impact on SOC (CS: 0.1 ton/ha (−0.12%), CSS: 2.03 ton/ha (−2.1%), and CSW: 2 ton/ha (−2.2%); Table S10). The SOC increase under treatment 9 mainly results from increased biomass (CS: 958 kg/ha (28%), CSS: 6140 kg/ha (+7%), and CSW: 4239 kg/ha (+46%);  $p$  < 0.05; Figure 8a; Table S12) and resultant residue accumulation. Additionally, the CSW experienced a decrease in soil respiration (344 kg/ha (−8%)), while CSS and CS rotations showed increased soil respiration (250 kg/ha (+6%) and 84 kg/ha (+2%), respectively;  $p$  < 0.05; Figure 8c; Table S11). The result confirmed that fertilization has a great impact on SOC sequestration. For instance, using the fuzzy analytical hierarchy process, Zahedifar [80] showed that soil N is highly significant when considering increasing soil SOC or biomass. Mohanty et al. [70] also reported a significant SOC sequestration with increased fertilization using the APSIM model. Adjusting the N application date to align with the crop's nutrient demand might improve nitrogen use efficiency (NUE) [98]. With better timing, the plants take up more N, leading to increased biomass and, consequently, higher levels of SOC. Additionally, with less fertilization, POC and DOC load tend to reduce, while with more fertilization, they tend to increase across rotations (from treatment

3 to treatments 5 and 10). Interestingly, CSW significantly reduces POC and DOC loads in treatment 9 (1.82 kg/ha (−21%) and 14 kg/ha (−20%), respectively), consistent with previous annual and seasonal analyses.

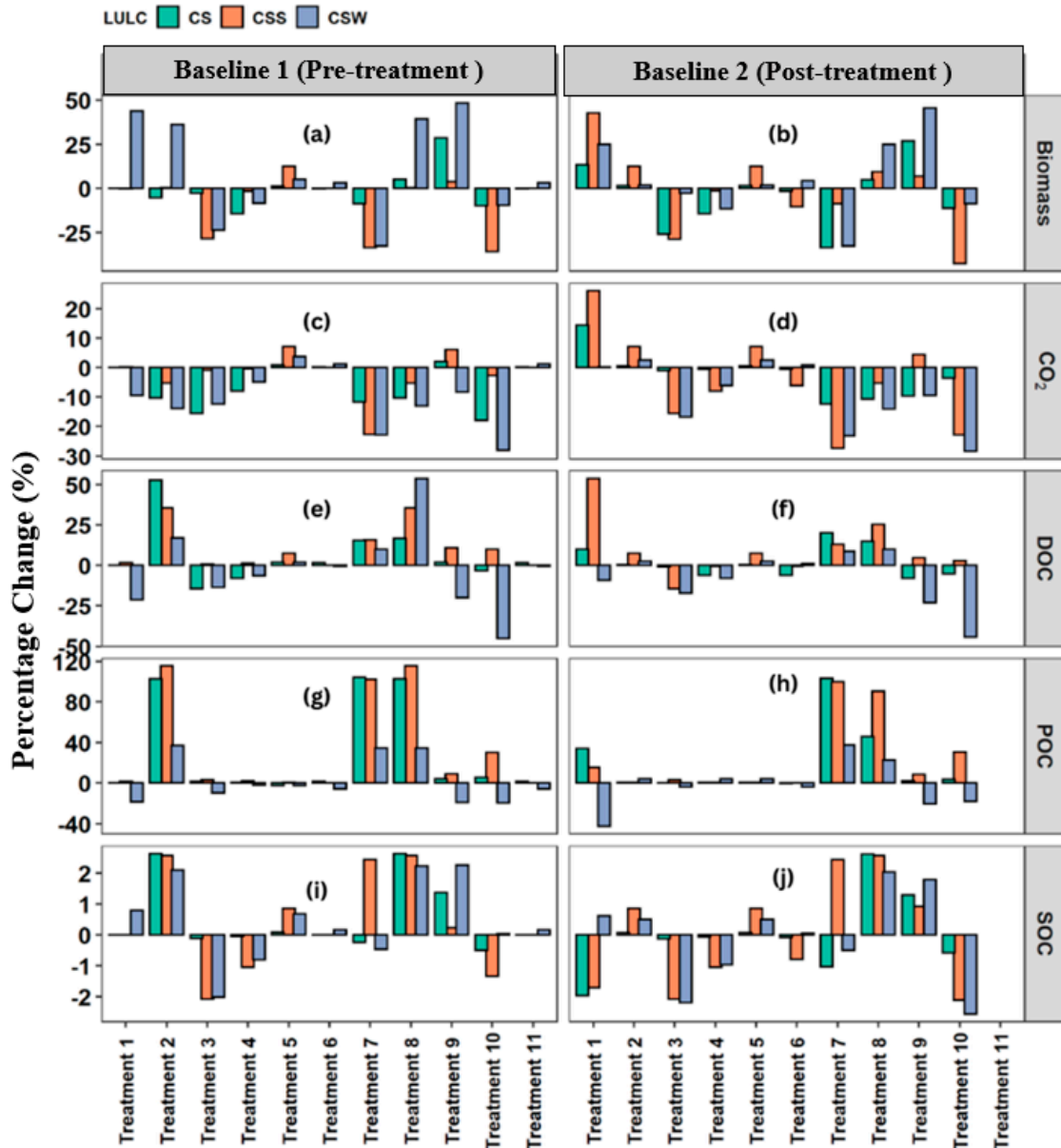


**Figure 8.** The average annual (2001–2020) percentage changes in (a,b) biomass, (c,d) soil respiration CO<sub>2</sub>, (e,f) DOC and (g,h) POC loads, and (i,j) SOC across three rotations for various treatments under baseline scenarios 1 and 2 (see Tables S10–S15 for details).

Under sub-category (1b), we found that treatment 8 has the largest SOC sequestration in all three rotations (CS: 2.74 ton/ha (+2.6%), CSS: 2.6 ton/ha (+2.6%), and CSW: 2 ton/ha (+2.1%);  $p < 0.05$ ; Figure 8i; Table S10) due to general increases in biomass and reduction in respiration. While POC and DOC losses rose, their extent (ranging from 2.8 to 28 kg/ha) in the three rotations was negligible compared to the sequestered SOC magnitude (>2 ton/ha; Figure 8c,e; Tables S10 and S11). Although soil respiration reduced for all rotations in treatment 7, SOC change was negative for CS (0.5 ton/ha (−0.24%)) and CSW (0.3 ton/ha (−0.5%)) due to reduced biomass but not for CSS rotation (2.4 ton/ha (+2.4%)), which might be attributable to its N-fixing ability (Figure 8i; Table S10;  $p < 0.05$ ). The decreased biomass under treatment 7 might be attributed to N stress [98–100], indicating the importance

of fertilization, even under NT, for biomass accumulation and its return to the soil as residue [68]. In a similar study, Huynh et al. [66] reported a significant reduction in maize yield under NT with a full irrigation system.

The sub-category (1c) analysis shows that SOC change was negative in both treatments except for CSW: 0.83 ton/ha (+0.8%; Figure 8i, Table S10) in treatment 1, which was consistent with increased biomass 5, 566 kg/ha (+44%; Figure 8a; Table S12;  $p < 0.05$ ). Despite full fertilization, CS and CSS growth was limited by other stresses such as water deficiency (no irrigation for this sub-category). The result also indicates that adding winter wheat to the corn–soybean rotation would potentially increase SOC due to increased biomass and reduced soil respiration, POC, and DOC loads with proper fertilization. As such, CSW rotation under treatment 1 can sequester SOC while decreasing losses through POC, DOC, and CO<sub>2</sub> emission.

### Tillage Effects

An examination of sub-category (2a) reveals that, under full fertilization and no irrigation, the comparison between CT and NT resulted in a biomass increase solely for the CSW rotation in both treatments, suggesting a water-stressed environment (Figure 8a;  $p < 0.05$ ). Nevertheless, SOC levels increased for all crop rotations in treatment 2 (Figure 8j;  $p < 0.05$ ), highlighting the importance of no-till practices in SOC sequestration. Farina et al. [101] reported consistent SOC sequestration under NT in maize-sunflower rotation using the EPIC model, although their study did not account for C losses. Olson et al. [63] also reported that tillage operation could increase residue oxidation and soil respiration, thereby increasing SOC losses. Arunrat [102] reported that practices supporting soil erosion or displacement result in SOC losses. The reduction in soil respiration (as depicted in Figure 8c; Refer to Table S11;  $p < 0.05$ ) coupled with enhanced biomass was the predominant element leading to elevated SOC storage under treatment 2. CSW under treatment 1 and all three rotations under treatment 2 are good candidates for SOC storage compared to the pre-treatment, indicating the importance of finding a suitable cover crop for C management [103].

An examination of sub-category (2b) reveals a general decline in SOC storage in both treatments with full irrigation and no fertilization, except for the CSS rotation in treatment 7. The primary cause of this reduction was a decrease in biomass across rotations, resulting from N stress. In both treatments, soil respiration was reduced, mainly because of lower residue input (Table S11;  $p < 0.05$ ). The changes in POC and DOC loads varied between the two treatments, with treatment 7 showing noticeable increases in POC and DOC loads (Figure 8e,g; Tables S10 and S11;  $p < 0.05$ ). No-till practices resulted in increased POC and DOC loads due to the accumulation of residue on the soil surface, where runoff and erosion transported OC downwards and to the streams. A similar finding was reported by Dou [67], who found a significant increase in POC and DOC loads due to increased surface residue under the NT system. Overall, the findings again highlight the significance of fertilization in both conservation tillage and no-till systems for SOC sequestration compared to the pre-treatment.

### Irrigation Effects

An evaluation of category (3a) reveals that no significant changes in SOC were observed for CS and CSS rotations in both treatments 1 and 6 (Figure 8i;  $p < 0.05$ ). In contrast, a slight increase in SOC was noted for CSW (+0.8% and +0.2%, respectively) in response to increased biomass. Interestingly, the CSW biomass with no irrigation in treatment 1 exceeded that of −50% irrigation in treatment 6 (Figure 8a). This outcome may result from nutrient leaching from winter wheat under irrigation during the wintertime with full fertilization. Concurrently, soil respiration for CSW in treatment 1 decreased as the lower soil moisture levels were less conducive for decomposition (Figure 8c; Table S11;  $p < 0.05$ ). Additionally, POC and DOC loads diminished due to reduced surface runoff and erosion caused by cover crops in treatment 1 (Figure 8e,g).

An evaluation of sub-category (3b) demonstrates that treatments 3 and 10, under CT without fertilization and regardless of irrigation levels, result in a significantly decreased biomass (Figure 8a; Table S12;  $p < 0.05$ ) and a decline in SOC sequestration (Figure 8i;  $p < 0.05$ ). Consequently, this led to decreased respiration across all three rotations and a consistent reduction in POC and DOC loads for the CSW rotation (Figure 8c,e,g; Tables S10 and S11;  $p < 0.05$ ). In contrast, we observed increased POC and DOC loads for the CSS rotation in both treatments compared to the pre-treatment, suggesting that incorporating an additional soybean crop into the corn–soybean rotation may lead to higher lateral C losses due to its low C: N ratio [94,95].

An examination of sub-category (3c) reveals that both NT systems can enhance SOC storage with full fertilization regardless of irrigation or not (Figure 8i; Table S10;  $p < 0.05$ ), attributed to increased biomass and the low oxidative nature of the NT systems [70]. As anticipated, adding irrigation led to increased biomass for CSW (+39%; Figure 8a;  $p < 0.05$ ) and decreased respiration (Figure 8c;  $p < 0.05$ ) in treatment 8. However, we observed a significant increase in POC and DOC loads in treatment 8 compared to treatment 2. This may be attributed to the water erosion of C-rich sediment due to irrigation.

### 3.4.2. Scenario 2 Analysis Fertilization Effects

The sub-category (1a) analysis revealed that treatments 5 and 9 increased SOC compared with current management practices (Table S2). In contrast, treatments 3 and 4 caused a decrease in SOC across all three rotations (Figure 8j; Table S13;  $p < 0.05$ ), consistent with the simulated changes in biomass (Figure 8b; Table S15;  $p$ -value  $< 0.05$ ). However, SOC losses through soil respiration and lateral losses differed between treatments 5 and 9. Treatment 5 showed an increase in all C variables across rotations (Figure 8f,h; Tables S13 and S14;  $p < 0.05$ ) compared with current management practices (Table S2). In contrast, treatment 9 indicated reduced soil respiration and DOC load for both CS and CSW and decreased POC load for CSW only (Figure 8d,f,h; Tables S13 and S14;  $p$ -value  $< 0.05$ ). These findings suggest that shifting the fertilization date enhances biomass and SOC, lowering CO<sub>2</sub> emissions and lateral C losses, as demonstrated in baseline 1 analysis. With decreased fertilization levels in treatments 3 and 4, most C budget components were reduced, emphasizing the significance of fertilization for SOC sequestration [104,105].

The sub-category (1b) analysis shows that under treatment 7, SOC sequestration increased only in the CSS rotation (+2.4%) compared with current management practices (Table S2). In contrast, treatment 8 led to increased SOC sequestration across all three rotations: CSS (+2.6%), CSW (+2%), and CS (+2.6%) (Figure 8j; Table S13;  $p$ -value  $< 0.05$ ). Treatment 8 exhibited a positive biomass increase for all rotations, while treatment 7 displayed the opposite due to zero fertilization (Figure 8b; Table S15;  $p$ -value  $< 0.05$ ). Both treatments resulted in lower CO<sub>2</sub> emissions across all three rotations (Figure 8d;  $p$ -value  $< 0.05$ ), attributable to the lower oxidation levels in the NT system [106]. POC and DOC loads increased significantly under treatments 7 and 8, as explained in previous sections (Figure 8f,h; Tables S13 and S14;  $p$ -value  $< 0.05$ ).

The sub-category (1c) analysis reveals that treatments 1 and 10 experienced significant SOC decreases (Figure 8j; Table S13;  $p$ -value  $< 0.05$ ) compared with current management practices (Table S2), except for CSW in treatment 1. There is an increase in biomass in all three rotations in treatment 1 due to full fertilization, while it decreased in treatment 10 due to zero fertilization (Figure 8b; Table S15;  $p$ -value  $< 0.05$ ). The SOC decrease for CS (−1.7%) and CSS (−2%) in treatment 1 can be attributed to the significant increase in soil respiration and POC and DOC loads (Figure 8d,f,h; Tables S13 and S14;  $p < 0.05$ ). Changes in POC and DOC loads varied across rotations in treatment 10, with CSS exhibiting increased POC and DOC loads while CSW showed decreased loads. This highlights that winter wheat can reduce lateral C losses with CT, as discussed earlier.

### Tillage Effects

An examination of sub-category (2a) shows consistent increases in SOC for all three rotations compared with current management practices (Table S2) in the NT system of treatment 2, resulting from increased biomass (Figure 8b,j; Tables S13 and S14;  $p < 0.05$ ). However, soil respiration and POC and DOC loads also increased (Figure 8d,f,h; Tables S13 and S14;  $p < 0.05$ ). Compared to treatment 2, the increase in biomass for all rotations was greater in treatment 1 with CT. However, SOC decreased due to significant  $\text{CO}_2$ , POC, and DOC losses for CS and CSS rotations, highlighting the substantial negative impact of CT on SOC losses. In a similar study, Begum et al. [107] reported a ~51% increase in SOC under NT with the proper fertilization level using the ECOSSE model. However, their study did not account for C losses.

A sub-category (2b) analysis shows that SOC decreased in treatments 3 and 7 across rotations (except for CSS in treatment 7; Figure 8j; Table S13;  $p < 0.05$ ) compared with current management practices (Table S2), consistent with the decline in biomass due to zero fertilization. Soil respiration also decreased as a result of N stress. However, SOC increased under CSS (+2.43%) in treatment 7 with NT, highlighting the importance of soybeans for N fixation [108]. In the NT system, POC and DOC loads (Figure 8f,h;  $p < 0.05$ ) significantly increased in treatment 7 across all rotations due to residue accumulation on the soil surface, where runoff and erosion occur. In contrast, no consistent pattern was observed for POC and DOC load changes in treatment 3 with CT where less surface residue accumulates.

### Irrigation Effects

An examination of sub-category (3a) reveals that while SOC decreased for CS and CSS and slightly increased for CSW in treatments 1 and 6 compared with current management practices (Table S2; Figure 8j; Table S13;  $p < 0.05$ ), the causes differed. In treatment 1, increased biomass led to higher SOC, while in treatment 6, decreased soil respiration and POC and DOC loads contributed to the net SOC increase (Figure 8b,d,j,h; Tables S13–S15;  $p < 0.05$ ). As observed in baseline 1 analysis, biomass significantly increased in treatment 1 with no irrigation but decreased with 50% less irrigation, indicating that irrigation may be a source of nutrient leaching. Increased soil respiration in the no irrigation treatment also supports this observation. With the 50% less irrigation treatment, changes in all variables were relatively small compared to other treatments.

A sub-category (3b) analysis reveals a consistent decrease in SOC for treatments 3 and 10 across rotations (Figure 8j; Table S13;  $p < 0.05$ ) due to reduced biomass caused by zero fertilization compared with current management practices (Table S2). As expected, soil respiration also decreased in both treatments (Figure 8d;  $p < 0.05$ ), suggesting the dominance of fertilization compared to irrigation in biomass accumulation and its return to the soil as residue. CSW tends to have a greater reduction of POC and DOC loads than other rotations, particularly in treatment 10 with no irrigation, which can be partially attributed to reduced soil erosion (Figure 8f,h; Tables S13 and S14). On the other hand, CSS showed increased POC and DOC in treatment 10, indicating distinct responses of soybean and winter wheat to zero irrigation treatment.

Examining sub-category (3a) reveals a consistent increase in SOC for treatments 2 and 8 across all rotations (Table S13;  $p < 0.05$ ) compared with current management practices (Table S2). Although both treatments experienced increased biomass due to full fertilization, soil respiration increased under treatment 2 but decreased under treatment 8 (Figure 8d; Table S14;  $p < 0.05$ ). It is suspected that with full irrigation, plants would absorb more nutrients from the soil, which would impede microbial activities. POC and DOC loads increased for both treatments across rotations, but treatment 8 had a greater magnitude, which might be attributed to increased runoff and erosion (Figure 8f,h; Tables S13 and S14). Interestingly, CSS increased POC and DOC loads more than other rotations, possibly due to the less protected soil surface and a higher decomposition rate.

### 3.5. Limitations and Future Directions

Previous studies using SWAT-C to simulate soil organic C dynamics considered only eroded C yield from an agricultural landscape (e.g., [45]) and vertical SOC distribution in the U.S. Cornbelt (e.g., [50]). Our research represents progress in testing the capacity of SWAT-C to simulate the impact of land use and various management practices on lateral C fluxes, both in dissolved and particulate forms, at the watershed scale, particularly within different corn-based rotations. However, we acknowledge that our modeling results, although compared with other studies, may be subject to discussion and carry significant uncertainty. This is primarily due to the lack of specific observational data regarding the various land-use types and management practice combinations that would allow us to validate the model results. As such, future assessments of SWAT-C at the site level, employing more detailed observational data, would provide a better understanding of SWAT-C's strengths and weaknesses in simulating both the lateral and vertical movements of eroded and leached C.

## 4. Conclusions

In our research, we employed a distributed eco-hydrological model known as SWAT-C to simulate the losses of soil organic carbon (SOC) via particulate OC (POC) and dissolved OC (DOC) loads into surface water. The study focused on a typical agricultural watershed in the Mid-Atlantic Region, i.e., the Upper Maurice River Watershed (UMRW) in New Jersey, USA. We used historical (2001–2020) streamflow and water quality records (specifically, sediment, POC, and DOC loads) from USGS to calibrate and validate the SWAT-C model to simulate SOC dynamics and POC and DOC transfer and transformation from landscape to stream networks. Simulations from 2001 to 2020 revealed that surface runoff contributed 65% to the yearly total DOC load, with lateral flow adding 30% and groundwater contributing a minor 5% within the watershed. An in-depth examination of land-use effects on average annual POC and DOC loads revealed that, in general, agricultural land-use types generated the highest levels of DOC and POC. In comparison, barren land produced the lowest DOC and POC loads, while forest and grassland land-use types yielded intermediate levels of DOC and POC. Concerning seasonal fluctuations, agricultural land-use types exhibited distinct DOC and POC load patterns compared to forest and grassland types, indicating management practices' dominant role in determining SOC losses. We concentrated on three primary crop rotations among various agricultural land-use types, including corn–soybean (CS), corn–soybean–soybean (CSS), and corn–soybean–winter wheat (CSW). Our findings revealed that the seasonal DOC load for the CSW rotation differed from those of CS and CSS, particularly during the spring and summer months. CSW generated significantly reduced DOC loads, a result of additional tillage activities post soybean harvest diminishing the accumulation of organic matter on the surface. In line with the annual findings, agricultural land-use types generally produced significantly higher POC loads compared to forests and grasslands across all seasons. This is because forests and grasslands experience less erosion due to better surface soil protection. The seasonal patterns of POC load varied among the agricultural land-use types. The CSW rotation protects the soil surface from erosion during winter wheat growth in the cold season. Conversely, the CSS rotation resulted in a higher POC load during winter, suggesting a tendency for soybean decomposition in colder seasons due to its low C: N ratio. The subsequent lack of adequate soil coverage may have contributed to sediment erosion.

We expanded our analysis to examine the effects of management practices on biomass accumulation, SOC changes, soil microbial respiration (i.e., CO<sub>2</sub> emissions), and lateral C losses (in the form of DOC and POC). We investigated various combinations of commonly used management practices, such as different levels of tillage, irrigation, and fertilization in the watersheds, to determine the most effective strategy for increasing SOC storage while reducing CO<sub>2</sub> emissions and lateral C losses. Simulations involving different treatments (combinations of varying levels of the three management practices) were compared with two baselines: (1) a pre-treatment baseline (no irrigation, tillage, or fertilization) and (2) a

post-treatment baseline (current management practices in the watershed). The results indicated that the highest SOC sequestration was achievable through a combination of full irrigation, no-till (NT), and full fertilization in the three rotations, compared with both baselines. Conversely, the most significant SOC depletion occurred when combining conservation tillage (CT) and no fertilization, regardless of the irrigation conditions in the two scenarios. Our research also indicated that incorporating a cover crop like winter wheat into the corn–soybean rotation could potentially enhance SOC through increased biomass and decreased soil respiration, POC, and DOC loads when properly fertilized. In conclusion, our study showcased the applicability of SWAT-C in quantifying lateral DOC and POC fluxes from agricultural watersheds to riverine ecosystems. It can also be employed for analyzing the impacts of land use and management practices on SOC changes. SWAT-C proves to be a valuable decision support tool for developing watershed C management plans.

**Supplementary Materials:** The following supporting information can be downloaded at: <https://www.mdpi.com/article/10.3390/w15203534/s1>. Figure S1. Percentage area of each land-use type in the Upper Maurice River Watershed (UMRW) in southern New Jersey. Figure S2. Monthly average evapotranspiration and snowmelt from 2000–2020 in the UMRW. Figure S3. Simulated versus observed daily (a) streamflow (b) sediment, (c) POC, and (d) DOC loads during the calibration (2001–2010) and validation (2011–2020) periods. Figure S4. Average monthly precipitation and temperature vs. DOC and POC load from 2001 to 2020. Figure S5. (a) Percentage contributions to DOC and (b) POC load during the fall, spring, winter, and summer seasons in the UMRW. Figure S6. Percentage contributions of surface runoff, lateral flow, and groundwater DOC load during the fall, spring, winter, and summer seasons in the UMRW. Figure S7. (a) Corn, (b) soybean, and (c) winter wheat calibrations. Observed values are obtained from USDA-NASS, while simulated values are obtained from SWAT’s output file. Table S1. Detailed land use types in the study area (excluding urban and water areas). Table S2. Management practices are concomitant with irrigation scheduling operations for corn and soybean in the SWAT model. Table S3. Calibrated model parameter values for the study watershed’s streamflow, sediment, POC, and DOC loads. Table S4. Model performance on daily streamflow, sediment, POC, and DOC loads during calibration (2001–2010) and validation (2011–2020) periods at USGS gauging station 01411500, Maurice River at Norma. Table S5. Model parameter uncertainty analysis results indicated by the p-factor and the r-factor for streamflow, sediment, POC, and DOC load simulations during calibration (2001–2010) and validation (2011–2020) at USGS gauging station 01411500, Maurice River at Norma. Table S6. Model parameter sensitivity analysis results for streamflow, sediment, POC, and DOC load simulations in the Upper Maurice River watershed. Table S7. Annual water yield, sediment, POC, and DOC loads over Upper Maurice River Watershed in New Jersey. Table S8. POC Tukey. Table S9. DOC Tukey. Table S10. 20-year annual average SOC (ton/ha) and POC load (kg/ha), along with percentage change (i.e., values in bracket) compared with the pre-treatment level under baseline 1 for three rotations and various treatments. Table S11. 20-year annual average DOC load (kg/ha) and soil respiration CO<sub>2</sub> (kg/ha), along with percentage change (i.e., values in bracket) compared with the pre-treatment level under baseline 1 for three rotations and various treatments. Table S12. 20-year annual average biomass (kg/ha) along with percentage change (i.e., values in bracket) compared with the pre-treatment level under baseline 1 for three rotations and various treatments. Table S13. 20-year annual average SOC (tons/ha) and POC load (kg/ha), along with percentage change (i.e., values in bracket) compared with the post-treatment level under baseline 2 for three rotations and various treatments. Table S14. 20-year annual average DOC load (kg/ha) and soil respiration CO<sub>2</sub> (kg/ha), along with percentage change (i.e., values in bracket) compared with the post-treatment level under baseline 2 for three rotations and various treatments. Table S15. 20-year annual average biomass (kg/ha), along with percentage change (i.e., values in bracket) compared with the post-treatment level under baseline 2 for three rotations and various treatments.

**Author Contributions:** Conceptualization, J.Q. and S.B.T.; methodology, J.Q. and S.B.T.; software, J.Q.; validation, S.B.T., S.G. and R.L.; formal analysis, S.B.T.; investigation, J.Q.; resources, S.G. and R.L.; data curation, J.Q.; writing—original draft preparation, S.B.T.; writing—review and editing, J.Q.; visualization, S.B.T.; supervision, S.G. and R.L.; project administration, J.Q.; funding acquisition, J.Q. All authors have read and agreed to the published version of the manuscript.

**Funding:** This research was funded by the U.S. Department of Agriculture (USDA), the National Institute of Food and Agriculture (2021-67019-33684 and 2023-67019-39221), and the National Aeronautics and Space Administration (NNX17AE66G and 80NSSC20K0060).

**Data Availability Statement:** The data presented in this study are available on request from the corresponding author.

**Conflicts of Interest:** The authors declare no conflict of interest.

## References

1. Wiesmeier, M.; Poeplau, C.; Sierra, C.A.; Maier, H.; Frühauf, C.; Hübner, R.; Kühnel, A.; Spörlein, P.; Geuß, U.; Hangen, E.; et al. Projected Loss of Soil Organic Carbon in Temperate Agricultural Soils in the 21st Century: Effects of Climate Change and Carbon Input Trends. *Sci. Rep.* **2016**, *6*, 32525. [[CrossRef](#)] [[PubMed](#)]
2. Winowiecki, L.; Vågen, T.G.; Massawe, B.; Jelinski, N.A.; Lyamchai, C.; Sayula, G.; Msoka, E. Landscape-Scale Variability of Soil Health Indicators: Effects of Cultivation on Soil Organic Carbon in the Usambara Mountains of Tanzania. *Nutr. Cycl. Agroecosyst.* **2016**, *105*, 263–274. [[CrossRef](#)]
3. Lal, R. Soil Carbon Sequestration to Mitigate Climate Change. *Geoderma* **2004**, *123*, 1–22. [[CrossRef](#)]
4. Magdoff, F.; Van Es, H. *Handbook Building Soils for Better Crops Ecological Management for Healthy Soils*, 4th ed.; Handbook Series 10; SARE: College Park, MD, USA, 2021.
5. Foley, J.A.; DeFries, R.; Asner, G.P.; Barford, C.; Bonan, G.; Carpenter, S.R.; Chapin, F.S.; Coe, M.T.; Daily, G.C.; Gibbs, H.K.; et al. Global Consequences of Land Use. *Science* **2005**, *309*, 570–574. [[CrossRef](#)] [[PubMed](#)]
6. Villarino, S.H.; Studdert, G.A.; Lateral, P. How Does Soil Organic Carbon Mediate Trade-Offs between Ecosystem Services and Agricultural Production? *Ecol. Indic.* **2019**, *103*, 280–288. [[CrossRef](#)]
7. Wei, X.; Shao, M.; Gale, W.; Li, L. Global Pattern of Soil Carbon Losses Due to the Conversion of Forests to Agricultural Land. *Sci. Rep.* **2014**, *4*, 4062. [[CrossRef](#)]
8. Ashagrie, Y.; Zech, W.; Guggenberger, G.; Mamo, T. Soil Aggregation, and Total and Particulate Organic Matter Following Conversion of Native Forests to Continuous Cultivation in Ethiopia. *Soil Tillage Res.* **2007**, *94*, 101–108. [[CrossRef](#)]
9. Kemanian, A.R.; Stöckle, C.O.; Huggins, D.R.; Viega, L.M. A Simple Method to Estimate Harvest Index in Grain Crops. *Field Crops Res.* **2007**, *103*, 208–216. [[CrossRef](#)]
10. Bai, Z.G.; Dent, D.L.; Olsson, L.; Schaepman, M.E. Proxy Global Assessment of Land Degradation. *Soil Use Manag.* **2008**, *24*, 223–234. [[CrossRef](#)]
11. Stockmann, U.; Adams, M.A.; Crawford, J.W.; Field, D.J.; Henakaarchchi, N.; Jenkins, M.; Minasny, B.; Mcbratney, A.B.; De Remy De Courcelles, V.; Singh, K.; et al. The Knowns, Known Unknowns and Unknowns of Sequestration of Soil Organic Carbon. *Ecosys. Environ.* **2013**, *164*, 80–99. [[CrossRef](#)]
12. Lal, R. Soil Carbon Sequestration Impacts on Global Climate Change and Food Security. *Science* **2004**, *304*, 1623–1627. [[CrossRef](#)]
13. Polyakov, V.O.; Lal, R. Soil Erosion and Carbon Dynamics under Simulated Rainfall. *Soil Sci.* **2004**, *169*, 590–599. [[CrossRef](#)]
14. Schreiber, J.D. Nutrient Leaching from Corn Residues under Simulated Rainfall. *J. Environ. Qual.* **1999**, *28*, 1864–1870. [[CrossRef](#)]
15. Gmach, M.R.; Cherubin, M.R.; Kaiser, K.; Cerri, C.E.P. Processes That Influence Dissolved Organic Matter in the Soil: A Review. *Sci. Agric.* **2020**, *77*, e20180164. [[CrossRef](#)]
16. Manninen, N.; Soenne, H.; Lemola, R.; Hoikkala, L.; Turtola, E. Effects of Agricultural Land Use on Dissolved Organic Carbon and Nitrogen in Surface Runoff and Subsurface Drainage. *Sci. Total Environ.* **2018**, *618*, 1519–1627. [[CrossRef](#)]
17. Alvarez-Cobelas, M.; Angeler, D.G.; Sánchez-Carrillo, S.; Almendros, G. A Worldwide View of Organic Carbon Export from Catchments. *Biogeochemistry* **2012**, *107*, 275–293. [[CrossRef](#)]
18. Zhang, X.; Izaurralde, R.C.; Arnold, J.G.; Williams, J.R.; Srinivasan, R. Modifying the Soil and Water Assessment Tool to Simulate Cropland Carbon Flux: Model Development and Initial Evaluation. *Sci. Total Environ.* **2013**, *463–464*, 810–822. [[CrossRef](#)] [[PubMed](#)]
19. Fatima, Z.; Ahmed, M.; Hussain, M.; Abbas, G.; Ul-Allah, S.; Ahmad, S.; Ahmed, N.; Ali, M.A.; Sarwar, G.; ul Haque, E.; et al. The Fingerprints of Climate Warming on Cereal Crops Phenology and Adaptation Options. *Sci. Rep.* **2020**, *10*, 1–21. [[CrossRef](#)]
20. Caverly, E.K. Ephemeral Organic Carbon Fluxes to the Chesapeake Bay from Ephemeral Organic Carbon Fluxes to the Chesapeake Bay from Agricultural Runoff on the Virginia Coastal Plain Agricultural Runoff on the Virginia Coastal Plain. Bachelor's Thesis, College of William and Mary, Williamsburg, VA, USA, 2012.
21. Regnier, P.; Friedlingstein, P.; Ciais, P.; Mackenzie, F.T.; Gruber, N.; Janssens, I.A.; Laruelle, G.G.; Lauerwald, R.; Luyssaert, S.; Andersson, A.J.; et al. Anthropogenic Perturbation of the Carbon Fluxes from Land to Ocean. *Nat. Geosci.* **2013**, *6*, 597–607. [[CrossRef](#)]
22. Ciais, P.; Borges, A.V.; Abril, G.; Meybeck, M.; Folberth, G.; Hauglustaine, D.; Janssens, I.A. The Impact of Lateral Carbon Fluxes on the European Carbon Balance. *Biogeosciences* **2008**, *5*, 1259–1271. [[CrossRef](#)]
23. Bondeau, A.; Smith, P.C.; Zaehle, S.; Schaphoff, S.; Lucht, W.; Cramer, W.; Gerten, D.; Lotze-campen, H.; Müller, C.; Reichstein, M.; et al. Modelling the Role of Agriculture for the 20th Century Global Terrestrial Carbon Balance. *Glob. Chang. Biol.* **2007**, *13*, 679–706. [[CrossRef](#)]

24. Dalzell, B.J.; Filley, T.R.; Harbor, J.M. The Role of Hydrology in Annual Organic Carbon Loads and Terrestrial Organic Matter Export from a Midwestern Agricultural Watershed. *GeCoA* **2007**, *71*, 1448–1462. [[CrossRef](#)]
25. Liu, J.; Sleeter, B.; Selmans, P.C.; Diao, J.; Zhou, Q.; Worstell, B.; Moritsch, M. Modeling Watershed Carbon Dynamics as Affected by Land Cover Change and Soil Erosion. *Ecol. Model.* **2021**, *459*, 109724. [[CrossRef](#)]
26. Lu, N.; Akujärvi, A.; Wu, X.; Liski, J.; Wen, Z.; Holmberg, M.; Feng, X.; Zeng, Y.; Fu, B. Changes in Soil Carbon Stock Predicted by a Process-Based Soil Carbon Model (Yasso07) in the Yanhe Watershed of the Loess Plateau. *Landsc. Ecol.* **2015**, *30*, 399–413. [[CrossRef](#)]
27. Xu, N.; Saiers, J.E.; Wilson, H.F.; Raymond, P.A. Simulating Streamflow and Dissolved Organic Matter Export from a Forested Watershed. *Water Resour. Res.* **2012**, *48*. [[CrossRef](#)]
28. Yadav, V.; Malanson, G.P.; Bekele, E.; Lant, C. Modeling Watershed-Scale Sequestration of Soil Organic Carbon for Carbon Credit Programs. *Appl. Geogr.* **2009**, *29*, 488–500. [[CrossRef](#)]
29. Rouhani, S.; Schaaf, C.L.; Huntington, T.G.; Choate, J. Simulation of Dissolved Organic Carbon Flux in the Penobscot Watershed, Maine. *Ecolhydro. Hydrobiol.* **2021**, *21*, 256–270. [[CrossRef](#)]
30. Futter, M.N.; Löfgren, S.; Köhler, S.J.; Lundin, L.; Moldan, F.; Bringmark, L. Simulating Dissolved Organic Carbon Dynamics at the Swedish Integrated Monitoring Sites with the Integrated Catchments Model for Carbon, INCA-C. *Ambio* **2011**, *40*, 906–919. [[CrossRef](#)]
31. Mayorga, E.; Seitzinger, S.P.; Harrison, J.A.; Dumont, E.; Beusen, A.H.W.; Bouwman, A.F.; Fekete, B.M.; Kroeze, C.; Van Drecht, G. Global Nutrient Export from Watersheds 2 (NEWS 2): Model Development and Implementation. *Environ. Model. Softw.* **2010**, *25*, 837–853. [[CrossRef](#)]
32. Arnold, J.G.; Moriasi, D.N.; Gassman, P.W.; Abbaspour, K.C.; White, M.J.; Srinivasan, R.; Santhi, C.; Harmel, R.D.; van Griensven, A.; Van Liew, M.W.; et al. SWAT: Model Use, Calibration, and Validation. *Trans. ASABE* **2012**, *55*, 1491–1508. [[CrossRef](#)]
33. Tijjani, S.B.; Giri, S.; Woznicki, S.A. Quantifying the Potential Impacts of Climate Change on Irrigation Demand, Crop Yields, and Green Water Scarcity in the New Jersey Coastal Plain. *Sci. Total Environ.* **2022**, *838*, 156538. [[CrossRef](#)] [[PubMed](#)]
34. EPA. What Climate Change Means for New Jersey. Available online: <https://19january2017snap-shot.epa.gov/sites/production/files/2016-09/documents/climate-change-nj.pdf> (accessed on 2 January 2022).
35. Cauller, S.J.; Carleton, G.B. Hydrogeology and Simulated Effects of Ground-Water Withdrawals, Kirkwood-Cohansey Aquifer System, Upper Maurice River Basin Area, New Jersey. *Sci. Investig. Rep.* **2006**. [[CrossRef](#)]
36. Barringer, J.L.; Kish, G.R.; Velch, A.J. *Corrosiveness of Ground Water in the Kirkwood-Cohansey Aquifer System of the New Jersey Coastal Plain*; Water-Resources Investigations Report 90-4180; New Jersey Department of Environmental Protection and Energy: West Trenton, NJ, USA, 1993.
37. Weather-Atlas New Jersey, USA—Climate Data and Average Monthly Weather | Weather Atlas. Available online: <https://www.weather-us.com/en/new-jersey-usa-climate> (accessed on 7 December 2021).
38. Taia, S.; Erraioui, L.; Arjald, Y.; Chao, J.; El Mansouri, B.; Scozzari, A. The Application of SWAT Model and Remotely Sensed Products to Characterize the Dynamic of Streamflow and Snow in a Mountainous Watershed in the High Atlas. *Sensors* **2023**, *23*, 1246. [[CrossRef](#)] [[PubMed](#)]
39. Wang, Z.; Cao, J.; Wang, Z. Spatial-Temporal Pattern Study on Water Conservation Function Using the SWAT Model. *Water Supply* **2021**, *21*, 3629–3642. [[CrossRef](#)]
40. Giri, S.; Arbab, N.N.; Lathrop, R.G. Assessing the Potential Impacts of Climate and Land Use Change on Water Fluxes and Sediment Transport in a Loosely Coupled System. *J. Hydrol.* **2019**, *577*, 123955. [[CrossRef](#)]
41. Singh, G.; Saraswat, D. Development and Evaluation of Targeted Marginal Land Mapping Approach in SWAT Model for Simulating Water Quality Impacts of Selected Second Generation Biofeedstock. *Environ. Model. Softw.* **2016**, *81*, 26–39. [[CrossRef](#)]
42. Fu, Q.; Yang, L.; Li, H.; Li, T.; Liu, D.; Ji, Y.; Li, M.; Zhang, Y. Study on the Optimization of Dry Land Irrigation Schedule in the Downstream Songhua River Basin Based on the SWAT Model. *Water* **2019**, *11*, 1147. [[CrossRef](#)]
43. Laurent, F.; Ruelland, D. Assessing Impacts of Alternative Land Use and Agricultural Practices on Nitrate Pollution at the Catchment Scale. *J. Hydrol.* **2011**, *409*, 440–450. [[CrossRef](#)]
44. Kemanian, A.R.; Julich, S.; Manoranjan, V.S.; Arnold, J.R. Integrating Soil Carbon Cycling with That of Nitrogen and Phosphorus in the Watershed Model SWAT: Theory and Model Testing. *Ecol. Model.* **2011**, *222*, 1913–1921. [[CrossRef](#)]
45. Zhang, X. Simulating Eroded Soil Organic Carbon with the SWAT-C Model. *Environ. Model. Softw.* **2018**, *102*, 39–48. [[CrossRef](#)]
46. Izaurrealde, R.C.; Williams, J.R.; McGill, W.B.; Rosenberg, N.J.; Jakas, M.C.Q. Simulating Soil C Dynamics with EPIC: Model Description and Testing against Long-Term Data. *Ecol. Model.* **2006**, *192*, 362–384. [[CrossRef](#)]
47. Du, X.; Zhang, X.; Mukundan, R.; Hoang, L.; Owens, E.M. Integrating Terrestrial and Aquatic Processes toward Watershed Scale Modeling of Dissolved Organic Carbon Fluxes. *Environ. Pollut.* **2019**, *249*, 125–135. [[CrossRef](#)]
48. Qi, J.; Zhang, X.; Lee, S.; Wu, Y.; Moglen, G.E.; McCarty, G.W. Modeling Sediment Diagenesis Processes on Riverbed to Better Quantify Aquatic Carbon Fluxes and Stocks in a Small Watershed of the Mid-Atlantic Region. *Carbon Balance Manag.* **2020**, *15*. [[CrossRef](#)]
49. Qi, J.; Du, X.; Zhang, X.; Lee, S.; Wu, Y.; Deng, J.; Moglen, G.E.; Sadeghi, A.M.; McCarty, G.W. Modeling Riverine Dissolved and Particulate Organic Carbon Fluxes from Two Small Watersheds in the Northeastern United States. *Environ. Model. Softw.* **2020**, *124*, 104601. [[CrossRef](#)]

50. Liang, K.; Qi, J.; Zhang, X.; Deng, J. Replicating Measured Site-Scale Soil Organic Carbon Dynamics in the U.S. Corn Belt Using the SWAT-C Model. *Environ. Softw.* **2022**, *158*, 105553. [[CrossRef](#)]
51. NJDEP. Land Use/Land Cover 2015 Update, Edition 20190128 (Land\_lu\_2015). Available online: <https://www.nj.gov/dep/gis> (accessed on 29 June 2022).
52. NOAA-NCEI Find a Station | Data Tools | Climate Data Online (CDO) | National Climatic Data Center (NCDC). Available online: <https://www.ncdc.noaa.gov/cdo-web/datatools/findstation> (accessed on 6 November 2021).
53. USDA-NRCS. Soil Survey Staff, Natural Resources Conservation Service, United States Department of Agriculture. Official Soil Series Descriptions. Available online: <https://datagateway.nrcs.usda.gov/GDGOrder.aspx> (accessed on 6 November 2021).
54. Neitsch, S.L.; Arnold, J.G.; Kiniry, J.R.; Williams, J.R. Soil, and Water Assessment Tool. User's Manual Version 2005, 476p. Available online: <https://swat.tamu.edu/media/1292/swat2005theory.pdf> (accessed on 27 September 2023).
55. Abbaspour, K.C.; Vaghefi, S.A.; Yang, H.; Srinivasan, R. Global Soil, Landuse, Evapotranspiration, Historical and Future Weather Databases for SWAT Applications. *Sci. Data* **2019**, *6*, 263. [[CrossRef](#)] [[PubMed](#)]
56. USDA. U.S. Geological Survey. Available online: <https://www.usgs.gov/products/data> (accessed on 29 June 2022).
57. Abbaspour, K.C. *SWAT-CUP 2012 SWAT Calibration and Uncertainty Programs*; Eawag: Dübendorf, Switzerland, 2012.
58. Nash, J.E.; Sutcliffe, J.V. River Flow Forecasting through Conceptual Models Part I—A Discussion of Principles. *J. Hydrol.* **1970**, *10*, 282–290. [[CrossRef](#)]
59. Tang, X.; Zhang, J.; Wang, G.; Jin, J.; Liu, C.; Liu, Y.; He, R.; Bao, Z. Uncertainty Analysis of Swat Modeling in the Lancang River Basin Using Four Different Algorithms. *Water* **2021**, *13*, 341. [[CrossRef](#)]
60. Moriasi, D.N.; Arnold, J.G.; Van Liew, M.W.; Bingner, R.L.; Harmel, R.D.; Veith, T.L. Model Evaluation Guidelines for Systematic Quantification of Accuracy in Watershed Simulations. *Trans. ASABE* **2007**, *50*, 885–900. [[CrossRef](#)]
61. Abbaspour, K.C.; Johnson, C.A.; van Genuchten, M.T. Estimating Uncertain Flow and Transport Parameters Using a Sequential Uncertainty Fitting Procedure. *Vadose Zone J.* **2004**, *3*, 1340–1352. [[CrossRef](#)]
62. Abbaspour, K.C.; Yang, J.; Maximov, I.; Siber, R.; Bogner, K.; Mieleitner, J.; Zobrist, J.; Srinivasan, R. Modelling Hydrology and Water Quality in the Pre-Alpine/Alpine Thur Watershed Using SWAT. *J. Hydrol.* **2007**, *333*, 413–430. [[CrossRef](#)]
63. Olson, K.R.; Gennadiyev, A.N.; Kovach, R.G.; Schumacher, T.E.; Olson, K.R.; Gennadiyev, A.N.; Kovach, R.G.; Schumacher, T.E. Comparison of Prairie and Eroded Agricultural Lands on Soil Organic Carbon Retention (South Dakota). *Open J. Soil Sci.* **2014**, *4*, 136–150. [[CrossRef](#)]
64. Lu, C.; Zhang, J.; Tian, H.; Crumpton, W.G.; Helmers, M.J.; Cai, W.J.; Hopkinson, C.S.; Lohrenz, S.E. Increased Extreme Precipitation Challenges Nitrogen Load Management to the Gulf of Mexico. *Commun. Earth Environ.* **2020**, *1*, 1–10. [[CrossRef](#)]
65. Culbertson, A.M.; Martin, J.F.; Aloysius, N.; Ludsins, S.A. Anticipated Impacts of Climate Change on 21st Century Maumee River Discharge and Nutrient Loads. *J. Great Lakes Res.* **2016**, *42*, 1332–1342. [[CrossRef](#)]
66. Huynh, H.T.; Hufnagel, J.; Wurbs, A.; Bellingrath-Kimura, S.D. Influences of Soil Tillage, Irrigation and Crop Rotation on Maize Biomass Yield in a 9-Year Field Study in Müncheberg, Germany. *Field Crops Res.* **2019**, *241*, 107565. [[CrossRef](#)]
67. Dou, F. Long-Term Tillage, Cropping Sequence, and Nitrogen Fertilization Effects on Soil Carbon and Nitrogen Dynamics A Dissertation. Ph.D. Thesis, Texas A&M University, College Station, TX, USA, 2005.
68. Rahmawati, R. Effect of Nitrogen Fertilizer on Growth and Yield of Maize Composite Variety Lamuru Creative Commons Attribution 4.0 International License. *Agrotech. J.* **2017**, *2*, 36–41. [[CrossRef](#)]
69. Halvorson, A.D.; Wienhold, B.J.; Black, A.L. Tillage, Nitrogen, and Cropping System Effects on Soil Carbon Sequestration. *Soil Sci. Soc. Am. J.* **2002**, *66*, 906–912. [[CrossRef](#)]
70. Mohanty, M.; Sinha, N.K.; Somasundaram, J.; McDermid, S.S.; Patra, A.K.; Singh, M.; Dwivedi, A.K.; Reddy, K.S.; Rao, C.S.; Prabhakar, M.; et al. Soil Carbon Sequestration Potential in a Vertisol in Central India- Results from a 43-Year Long-Term Experiment and APSIM Modeling. *Agric. Syst.* **2020**, *184*, 102906. [[CrossRef](#)]
71. Olson, K.R. Soil Organic Carbon Sequestration, Storage, Retention and Loss in U.S. Croplands: Issues Paper for Protocol Development. *Geoderma* **2013**, *195–196*, 201–206. [[CrossRef](#)]
72. Lasanta, T.; Mosch, W.; Pérez-Rontomé, M.C.; Navas, A.; Machín, J.; Maestro, M. Effects of Irrigation on Water Salinization in Semi-Arid Environments.: A Case Study in Las Bardenas, Spain. *Cuad. Investig. Geográf.* **2002**, *28*, 7–13. [[CrossRef](#)]
73. Li, M.; Peng, C.; Wang, M.; Xue, W.; Zhang, K.; Wang, K.; Shi, G.; Zhu, Q. The Carbon Flux of Global Rivers: A Re-Evaluation of Amount and Spatial Patterns. *Ecol. Indic.* **2017**, *80*, 40–51. [[CrossRef](#)]
74. Wallin, M.B.; Weyhenmeyer, G.A.; Bastviken, D.; Chmiel, H.E.; Peter, S.; Sobek, S.; Klemetsson, L. Temporal Control on Concentration, Character, and Export of Dissolved Organic Carbon in Two Hemiboreal Headwater Streams Draining Contrasting Catchments. *J. Geophys. Res. Biogeosci.* **2015**, *120*, 832–846. [[CrossRef](#)]
75. Glossner, K.; Lohse, K.A.; Appling, A.P.; Cram, Z.; Murray, E.; Godsey, S.E.; VanVactor, S.; McCorkle, E.P.; Seyfried, M.; Pierson, F.B. Long-Term Suspended Sediment and Particulate Organic Carbon Yields from the Reynolds Creek Experimental Watershed and Critical Zone Observatory. *Hydrol. Process* **2022**, *36*, e14484. [[CrossRef](#)]
76. Michalzik, B.; Kalbitz, K.; Park, J.H.; Solinger, S.; Matzner, E. Fluxes and Concentrations of Dissolved Organic Carbon and Nitrogen—a Synthesis for Temperate Forests. *Biogeochemistry* **2001**, *52*, 173–205. [[CrossRef](#)]
77. Anguria, P.; Chemining'wa, G.N.; Onwonga, R.N.; Ugen, M.A. Decomposition and Nutrient Release of Selected Cereal and Legume Crop Residues. *J. Agric. Sci.* **2017**, *9*, 108. [[CrossRef](#)]

78. Reis, E.M.; Baruffi, D.; Remor, L.; Zanatta, M. Decomposition of Corn and Soybean Residues under Field Conditions and Their Role as Inoculum Source. *Summa Phytopathol.* **2011**, *37*, 65–67. [[CrossRef](#)]
79. Lupwayi, N.Z.; Clayton, G.W.; O'donovan, J.T.; Harker, K.N.; Turkington, T.K.; Soon, Y.K. Nitrogen Release during Decomposition of Crop Residues under Conventional and Zero Tillage. *Can. J. Soil Sci.* **2006**, *86*, 11–19. [[CrossRef](#)]
80. Zahedifar, M. Feasibility of Fuzzy Analytical Hierarchy Process (FAHP) and Fuzzy TOPSIS Methods to Assess the Most Sensitive Soil Attributes against Land Use Change. *Environ. Earth Sci.* **2023**, *82*, 248. [[CrossRef](#)]
81. Millennium Ecosystem Assessment Panel. *Ecosystems and Human Well-Being—Synthesis: A Report of the Millennium Ecosystem Assessment*; Island Press: Washington, DC, USA, 2005. Available online: <https://edepot.wur.nl/45159> (accessed on 27 September 2023).
82. Vona, I.; Palinkas, C.M.; Nardin, W. Sediment Exchange Between the Created Saltmarshes of Living Shorelines and Adjacent Submersed Aquatic Vegetation in Chesapeake Bay. *Front. Mar. Sci.* **2021**, *8*, 1348. [[CrossRef](#)]
83. Gittman, R.K.; Peterson, C.H.; Currin, C.A.; Joel Fodrie, F.; Piehler, M.F.; Bruno, J.F. Living Shorelines Can Enhance the Nursery Role of Threatened Estuarine Habitats. *Ecol. Appl.* **2016**, *26*, 249–263. [[CrossRef](#)]
84. Glover, J.D.; Culman, S.W.; DuPont, S.T.; Broussard, W.; Young, L.; Mangan, M.E.; Mai, J.G.; Crews, T.E.; DeHaan, L.R.; Buckley, D.H.; et al. Harvested Perennial Grasslands Provide Ecological Benchmarks for Agricultural Sustainability. *Agric. Ecosyst. Environ.* **2010**, *137*, 3–12. [[CrossRef](#)]
85. Jackson, R.B.; Canadell, J.; Ehleringer, J.R.; Mooney, H.A.; Sala, O.E.; Schulze, E.D. A Global Analysis of Root Distributions for Terrestrial Biomes. *Oecologia* **1996**, *108*, 389–411. [[CrossRef](#)]
86. Department of Primary Industries and Regional Development. Soil Organic Matter—Frequently Asked Questions (FAQs). Agriculture and Food. Available online: <https://www.agric.wa.gov.au/soil-carbon/soil-organic-matter-fre-quently-asked-questions-faqs> (accessed on 17 October 2022).
87. Bowering, K.L.; Edwards, K.A.; Prestegaard, K.; Zhu, X.; Ziegler, S.E. Dissolved Organic Carbon Mobilized from Organic Horizons of Mature and Harvested Black Spruce Plots in a Mesic Boreal Region. *Biogeosciences* **2020**, *17*, 581–595. [[CrossRef](#)]
88. Pasricha, N.S. Conservation Agriculture Effects on Dynamics of Soil C and N under Climate Change Scenario. *Adv. Agron.* **2017**, *145*, 269–312. [[CrossRef](#)]
89. Sobczak, W.V.; Findlay, S. Variation in Bioavailability of Dissolved Organic Carbon among Stream Hyporheic Flowpaths. *Ecology* **2002**, *83*, 3194–3209. [[CrossRef](#)]
90. Siemens, J. Dissolved Organic Matter Induced Denitrification in Subsoils and Aquifers? Cite This Paper Related Papers. *Geoderma* **2003**, *113*, 253–271. [[CrossRef](#)]
91. NASA. Temperate Deciduous Forest: Mission: Biomes. Available online: <https://earthobservatory.nasa.gov/bi-ome/biotemperate.php> (accessed on 31 March 2023).
92. Ma, W.; Tang, S.; Dengzeng, Z.; Zhang, D.; Zhang, T.; Ma, X. Root Exudates Contribute to Belowground Ecosystem Hotspots: A Review. *Front. Microbiol.* **2022**, *13*, 937940. [[CrossRef](#)] [[PubMed](#)]
93. Kelly, V.; Stets, E.G.; Crawford, C. Long-Term Changes in Nitrate Conditions over the 20th Century in Two Midwestern Corn Belt Streams. *J. Hydrol.* **2015**, *525*, 559–571. [[CrossRef](#)]
94. Begum, N.; Guppy, C.; Herridge, D.; Schwenke, G. Influence of Source and Quality of Plant Residues on Emissions of N<sub>2</sub>O and CO<sub>2</sub> from a Fertile, Acidic Black Vertisol. *Biol. Fertil. Soils* **2014**, *50*, 499–506. [[CrossRef](#)]
95. Martens, D.A. Plant Residue Biochemistry Regulates Soil Carbon Cycling and Carbon Sequestration. *Soil Biol. Biochem.* **2000**, *32*, 361–369. [[CrossRef](#)]
96. Liu, T.; Chen, Z.; Rong, L.; Duan, X. Land-Use Driven Changes in Soil Microbial Community Composition and Soil Fertility in the Dry-Hot Valley Region of Southwestern China. *Microorganisms* **2022**, *10*, 956. [[CrossRef](#)] [[PubMed](#)]
97. Lal, R. Soil Erosion and Carbon Dynamics. *Soil Tillage Res.* **2005**, *81*, 137–142. [[CrossRef](#)]
98. Page, K.L.; Dalal, R.C.; Reeves, S.H.; Wang, W.J.; Jayaraman, S.; Dang, Y.P. Changes in Soil Organic Carbon and Nitrogen after 47 Years with Different Tillage, Stubble and Fertiliser Management in a Vertisol of North-Eastern Australia. *Soil Res.* **2020**, *58*, 346–356. [[CrossRef](#)]
99. Timmons, D.R.; Baker, J.L. Recovery of Point-Injected Labeled Nitrogen by Corn as Affected by Timing, Rate, and Tillage. *Agron. J.* **1991**, *83*, 850–857. [[CrossRef](#)]
100. Li, Y.; Li, J.; Gao, L.; Tian, Y. Irrigation Has More Influence than Fertilization on Leaching Water Quality and the Potential Environmental Risk in Excessively Fertilized Vegetable Soils. *PLoS ONE* **2018**, *13*, e0204570. [[CrossRef](#)] [[PubMed](#)]
101. Farina, R.; Seddaiu, G.; Orsini, R.; Steglich, E.; Roggero, P.P.; Francaviglia, R. Soil Carbon Dynamics and Crop Productivity as Influenced by Climate Change in a Rainfed Cereal System under Contrasting Tillage Using EPIC. *Soil Tillage Res.* **2011**, *112*, 36–46. [[CrossRef](#)]
102. Arunrat, N.; Sereenonchai, S.; Kongsurakan, P.; Hatano, R. Soil Organic Carbon and Soil Erodibility Response to Various Land-Use Changes in Northern Thailand. *Catena* **2022**, *219*, 106595. [[CrossRef](#)]
103. Ellmer, F.; Baumecker, M. 65 Years Long-Term Experiments at Thyrow. Results for Sustainable Crop Production at Sandy Soils. *Arch. Agron. Soil* **2010**, *21*, 521–531. [[CrossRef](#)]
104. Preza-Fontes, G.; Miller, H.; Camberato, J.; Roth, R.; Armstrong, S. Corn Yield Response to Starter Nitrogen Rates Following a Cereal Rye Cover Crop. *Crop Forage Turfgrass Manag.* **2022**, *8*, e20187. [[CrossRef](#)]

105. Havlin, J.L.; Beaton, J.D.; Tisdale, S.L.; Nelson, W.L. *Soil Fertility and Fertilizers: An Introduction to Nutrient Management*; Pearson: London, UK, 1999.
106. Olson, K.R. Impacts of Tillage, Slope, and Erosion on Soil Organic Carbon Retention. *Soil Sci.* **2010**, *175*, 562–567. [[CrossRef](#)]
107. Begum, K.; Zornoza, R.; Farina, R.; Lemola, R.; Álvaro-Fuentes, J.; Cerasuolo, M. Modeling Soil Carbon Under Diverse Cropping Systems and Farming Management in Contrasting Climatic Regions in Europe. *Front. Environ. Sci.* **2022**, *10*, 139. [[CrossRef](#)]
108. Van Vugt, D.; Franke, A.C.; Giller, K.E. Understanding Variability in the Benefits of N<sub>2</sub>-Fixation in Soybean-Maize Rotations on Smallholder Farmers' Fields in Malawi. *Agric. Ecosyst. Environ.* **2018**, *261*, 241. [[CrossRef](#)] [[PubMed](#)]

**Disclaimer/Publisher's Note:** The statements, opinions and data contained in all publications are solely those of the individual author(s) and contributor(s) and not of MDPI and/or the editor(s). MDPI and/or the editor(s) disclaim responsibility for any injury to people or property resulting from any ideas, methods, instructions or products referred to in the content.